DEVELOPMENT OF A NOVEL CATIONIC POLYMER-BASED IN-SITU GELLED ACID SYSTEM THAT IMPROVES ACID DIVERSION IN A HETEROGENEOUS CARBONATE RESERVOIR

A Thesis

by

ABHISHEK SARMAH

Submitted to the Office of Graduate and Professional Studies of
Texas A&M University
in partial fulfillment of the requirements for the degree of

MASTER OF SCIENCE

Chair of Committee,	Hisham Nasr-El-Din
Committee Members,	Jerome Schubert
	Mahmoud El-Halwagi
Head of Department,	Jeff Spath

December 2018

Major Subject: Petroleum Engineering

ABSTRACT

Viscosified acid systems have been used for acid diversion in heterogeneous carbonate reservoirs for several decades. However, the anionic polymers used in these systems are difficult to clean post treatment, leading to formation damage. This work evaluates a new cationic-polymer acid system with self-breaking ability for application as an acid diverter in carbonate reservoirs.

The apparent viscosities of the live and the partially neutralized acids at pH from 0 to 4.5 were measured as a function of the shear rate (1 to 1,000 s^{-1}). The effects of salinity and temperature (80 to 250°F) on the rheological properties of the acid system were also studied. The viscoelastic properties (G' and G") of the gelled acid system were evaluated using an oscillatory rheometer. Single coreflood experiments were conducted on Indiana limestone cores to study the nature of diversion caused by the polymer-acid system. The impact of permeability contrast on the process of diversion was investigated by conducting dual coreflood experiments on Indiana limestone cores which had a permeability contrast of 1.5-20. CT scans were conducted to study the propagation of wormhole post acid injection for both single and dual corefloods.

The live acid system (5 wt% HCl and 2.5 vol% polymer concentration) displayed a non-Newtonian shear thinning behavior with the viscosity declining from 117 to 19.4 cp when the shear rate increased from 10 to 500 s^{-1} at 250°F. Spent acid tests showed an increase in viscosity once the pH reached 2. The viscosity of the system increased from 117 cp at 10 s^{-1} at pH 0 to 185.8 cp at pH 2. The gel exhibited a strong elastic behavior

(G'- 5.18 Pa at 1 s^{-1}). The viscosity of the system continued to increase until it broke down without a breaker to 69 cp (at 250^{o}F and 10 s^{-1}) at a pH of 4.8, providing a self-breaking system which prevents formation damage due to polymer precipitation. Coreflood studies indicated that the wormhole propagation and the diversion processes are dependent on the temperature and the flow rate. There was no indication of any damage caused by the system to the cores.

The strong elastic nature of the gel generated by the partially neutralized acid system proves its suitability as a candidate for use as a diverting agent. The system offers an improvement over existing polymer-based acid systems because of its self-breaking ability and lack of precipitation, thus preventing formation damage.

DEDICATION

To my parents, brother and my friends.

ACKNOWLEDGEMENTS

I would like to express my gratitude to my advisor, Dr. Hisham A. Nasr-El-Din, for granting me the opportunity to carry out this research. His continuous support and encouragement proved to be the shining light as I navigated this journey.

I would like to thank my committee members, Dr. Jerome Schubert, and Dr. Mahmoud El-Halwagi, for their guidance during my research. I am also thankful to Dr. Jennifer Jackson and Dr. Anuradee (Oat) Witthayapanyanon from BASF Global Oilfield Solutions for their feedback that played a large role in shaping the direction of the research.

Thanks also go to Dr. Ahmed Ibrahim for mentoring me during my graduate studies. I appreciate the efforts of Ahmed Hanafy and Manayer Q. Al-Mujalhem for helping me with the CT scan image processing.

I am extremely grateful to my colleagues for making this time at Texas A&M University a wonderful experience. Special thanks to Harsha, Sneha, and Raja for their continuous support and discussions.

Finally, thanks to my mother and father for their encouragement without which I would never have had the courage to overcome the obstacles and pursue my dream. Last but not the least, I thank my brother for his support. This journey would not have been possible without everyone's help and encouragement.

CONTRIBUTORS AND FUNDING SOURCES

Contributors

This study was supervised by a thesis committee of Dr. Hisham A. Nasr-El-Din and Dr. Jerome Schubert of the Harold Vance Department of Petroleum Engineering and Dr. Mahmoud El-Halwagi of the Artie McFerrin Department of Chemical Engineering.

All other work on the viscometer and coreflood studies for the thesis were conducted by the student independently.

Funding Sources

This work was made possible in part by BASF Corporation under the project number 28-402267-00003.

NOMENCLATURE

A	cross-sectional area, cm^2
ACS	American Chemical Society
CT	computed tomography
ΔP	pressure drop across the core, atm
DI	de-ionized water
ft	feet
G’	elastic modulus, Pa
G”	viscous modulus, Pa
γ	shear rate, s^{-1}
HP/HT	high pressure – high temperature
ICP-OES	Inductively Coupled Plasma Optical Emission Spectroscopy
in	inch
K	power-law constant
k	permeability, Darcy
L_0	length of the core, cm
μ	fluid viscosity, cp
n	power-law index
ϕ	porosity, vol%
psi	pounds per square inch
PV	pore volume, cm^3

Q	flow rate, cm^3/min
ρ	density of de-ionized water, g/cm^3
V_{bulk}	volume of the core, cm^3
W_{dry}	dry weight of the core, g
W_{sat}	saturated weight of the core, g
XRD	X Ray Diffraction

TABLE OF CONTENTS

Page

LIST OF FIGURES

Page

LIST OF TABLES

Page

CHAPTER I

INTRODUCTION

The demand for energy has only increased in recent years as more and more nations aspire to a greater standard of living. Even as unconventional energy sources such as solar, wind etc. have gained popularity in recent times, oil and gas is still responsible for satisfying the majority of the world's energy demand. Thus, optimization for improving the recovery of hydrocarbons in underground reservoirs is a continued endeavor.

Hydrocarbon reservoirs, which are mineralogically either sandstones or carbonates are characterized by their porosity and permeability. It is observed that over the course of production from a reservoir the porosity and the permeability declines. This is known as formation damage and it occurs due to a plugging of pore spaces and pore throats. The plugging occurs due to a deposit of organic and mineral matter (Muecke 1982). This deposition of plugging material occurs during the various stages of well life such as drilling, cementing, workover, production, and stimulation (McLeod 1984).

Damage during drilling typically occurs by the invasion of drilling mud into the permeable formation. The mud filtrates lead to the swelling and migration of the clays present in the formation (Reed 1989). Cementing operations are carried out by pumping a cement slurry into the well to provide well bore stability through casing or to isolate a particular zone. These operations lead to influx of cement particles into formation and

causes the precipitation of calcium silicate and calcium hydroxide which leads to a decline in the permeability of the formation.

Large pressure drawdowns during production often cause migration of fines, particularly in sandstone reservoirs leading to plugging of the pore throats. Precipitation of fines can also be induced by HF / HCl injection (Bryant and Buller 1990). Completion jobs such as perforations lead to intrusion of debris and crushed fines into the formation (Klotz et al. 1974). Other completion jobs such as gravel packing for sand control involve the usage of gravel slurry that can squeeze pipe dope and scale into the formation causing high pressure drop (Houchin et al. 1988). Chemical treatments such as scale inhibitors and corrosion inhibitors also lead to formation damage by altering the wettability of the formation and inhibiting production. Acid injection into the reservoir often induces asphaltene precipitation and reduction of reservoir permeability. Asphaltene and wax deposition is also observed when colder treatment fluids are injected into the system (Leontaritis 1989). Thus, almost all operations carried out in a well's lifetime lead in one way or the other to formation damage in the reservoir. This damage is quantified by the skin factor; higher the skin factor the greater is the formation damage.

Matrix acidizing is one of the more conventional methods for removal of formation damage. It has been in use since the 1890s in the oil and gas industry and was initiated by the Standard Oil Company who patented the use of HCl to stimulate carbonate formations. Matrix acidizing typically involves the injection of a stimulating fluid (usually acids such as Hydrochloric Acid) at a pressure lower than the fracture pressure of the formation. The objective of matrix acidizing in sandstone reservoirs is to remove near wellbore damage

in a region of 1-3 ft from the perforation. While in carbonate reservoirs, the objective of such a treatment is to generate conductive channels, "wormholes" that bypass the damaged zone that exists up to 20 ft from the perforation and increase the permeability of the formation (Coulter and Jennings 1999).

Proper fluid placement is crucial for acid treatment design in both carbonate and sandstone reservoirs. In absence of an appropriate diversion method during matrix acidizing in a heterogeneous reservoir, the acid enters the higher permeability zones following the path of least resistance and bypasses the lower permeability zones altogether. Thus, if an efficient acid placement technique is absent, the high permeability effectively becomes the sink for the acid and the entire treatment process can be rendered ineffective (Nasr-El-Din et al. 2007). The diverters employed in the industry can be broadly categorized into two main categories: mechanical, and chemical isolation.

Mechanical isolation techniques are an easy way to ensure that the stimulating fluid enters areas they would not travel into naturally by controlling the fluid entry point at the wellbore. These techniques ensure that the path of least resistance is mechanically blocked from the fluid and it has no alternative but to flow through the only other path present (Kalfayan and Martin 2009). Various options exist to ensure isolate a zone and control the fluid entry into the reservoir such as bridge plugs, packers, ball sealers, coiled tubing etc. It is important to note that these isolation techniques are only helpful for diversion in the wellbore, and these techniques do nothing to prevent the flow of fluids inside the formation.

Chemical diversion techniques allow for diversion of stimulating fluids inside the reservoir. The essence of chemical diversion has remained the same since its inception in 1930's, i.e. a temporary blocking effect is created which is safely cleaned up after the treatment. The initial attempts for chemical diversion involved injecting calcium chloride ($CaCl_2$) with acid increasing the fluid viscosity and allowing the acid to contact the lower permeability zones. Modern day chemical diverters include: polymers, viscoelastic surfactants, foam, oil-soluble resins etc. These materials increase the effective viscosity and plug the wormhole reducing the fluid injection rate.

Polymer based systems are used for plugging the high permeability zones with a high viscosity gel. These systems can be broadly classified into two main categories: Gelled Acid Systems, and In-Situ Gelled Acid Systems. The difference between the two systems is that the gelled acid systems are already activated at the surface. Thus, when this acid system reaches the formation, the viscosity against both the high and the low permeability zones is identical and the volume of fluid which enters a zone would be determined by the permeability of the zone. The in-situ gelled acid on the other hand, increases in viscosity inside the formation. The acid enters the higher permeability zone initally, gets spent and an increase in viscosity occurs creating an injectivity contrast. This contrast generated offers resistance to the subsequent acid and diverts it to the lower permeability regions. The other advantage it offers is that because stimulation and diversion occurs simultaneously, lesser number of acid injection stages are required. However, these systems leave residues after the gels break, potentially eliminating the effects of stimulation by damaging the matrix (Lynn and Nasr-El-Din 2001).

Polymer based acid systems offers a viable method to achieve diversion in carbonate reservoirs. However, the associated problems of precipitation of polymers impairing the formation permeability is a major cause of concern. The current study deals with a novel cationic polymer-based acid system that improves diversion in carbonates while addressing the typical issue of polymer deposition at the same time.

CHAPTER II

LITERATURE REVIEW

Numerous studies have been conducted in the past, where an acid was viscosified with a polymer. The initial usage of such a polymer-acid system was to carry out fracture-acidizing. The usage of a polymer system offered numerous advantages: acid retardation, increased fracture width to decrease the area/volume ration, and improved leak-off control (Church et al. 1981). Field tests indicated that production stimulation resulting from fracture acidizing is enhanced by the use of acid gelling agents (Church et al. 1981, Norman et al. 1984, Johnson et al. 1988).

The usage of acid-gel systems for matrix acidizing has gained grounds in the last 3 decades. Bazin (1999) reported that gelled acid systems are highly effective in removing formation damage, particularly in horizontal wells where mechanical isolation techniques such as isolation packers or ball sealers are ineffective. Polymer based acid systems consist of an acid or acid blend (typically HCl), a polymer, a crosslinker, and a breaker. The polymer is usually a partially hydrolyzed polyacrylamide based and has carboxylic group which crosslink with iron or zirconium at a pH between 2 and 4 (Deysarkar et al. 1984). On reaction with the carbonate in the formation, the live acid starts crosslinking after it reaches a pH of greater than 2. An increase in viscosity of the spent acid occurs and the acid blocks the treated zone. This diverts the next stage of live acid into the untreated zones. The breaking agent activates at a pH of 4 and reverts the system to a lower viscosity fluid (MaGee et al. 1997, Hill 2005).

Conway et al. (1999) measured the impact of temperature on the reaction rates of regular and gelled HCl at varying concentrations of Ca^{2+} and Mg^{2+}. It was observed that the acid diffusion was directly related to temperature and acid concentration and inversely to the Ca^{2+} and Mg^{2+} concentrations. Lower acid diffusivity was observed for the gelled acid systems. Lakatos and Lakatos-Szabó (2004) observed that the increase in silicate content in a double network of crosslinked, high molecular weight, partially hydrolyzed polyacrylamide and polysilicate gel reduced the diffusion coefficient of H^+ ions. The reaction of in-situ gelled acid with calcite was mass transfer limited up to a rotational speed of 1,000 rev/min and surface transfer limited above this value at 150^{o}F. The presence of crosslinker decreased the rate of calcite dissolution in both mass transfer and surface reaction limited regimes (Rabie et al. 2011).

Different coreflood studies have been conducted in the past to simulate the matrix acidizing that occurs when gelled acids are injected into the formation. Taylor and Nasr-El-Din (2003) studied 3 formulations of in-situ gelled acids and observed that the systems caused an irreversible reduction of carbonate rock permeability. The primary cause of reduction in permeability was attributed to the polymer used. Lynn and Nasr-El-Din (2001) stated that the iron based crosslinker which is typically used in an in-situ gelled acid system precipitated along with the polymer when injected into a carbonate core.

Gomaa and Nasr-El-Din (2010 a) studied the rheological properties of the in-situ gelled acid extensively. The acid system displayed a non-Newtonian shear thinning behavior. Acid spending studies indicated that the acid displayed two distinct regimes: a pure viscous behavior at pH below 2 where the viscous modulus (G") was dominant; and

a semi-solid elastic behavior at pH greater than 2 with a significant increase in elastic modulus (G') as compared to G" values. Gomaa (2010 b) observed that an initial acid concentration of 5 wt% HCl was ideal for the system to achieve the maximum increase in viscosity at the crosslinking pH of 2. Concentration of salts was also found to have a major detrimental impact on the system viscosity and as such it was recommended to prepare these acids in fresh or low salinity waters. Parallel coreflood studies conducted by Gomaa et al (2011) indicated that injection rate played a significant role in determining the efficiency of the coreflood. At low flow rates, plugging was observed to have taken place on the injection face; while at high injection rates, the acid system could not generate a viscous plug strong enough to divert acid into the lower permeability core. A permeability contrast of 1:2 was determined to have provided the maximum diversion enhancing permeability in both cores.

Abdel Fatah et al. (2008) reported that the crosslinker and the corrosion inhibitor employed in the in-situ gelled acid impacted the gelation. Aluminum based crosslinkers were found to have formed a gel at a pH higher than that observed with the iron-based one. Corrosion inhibitors were found to reduce the pH at gelation for iron based cross-linker and increase the gelation pH for aluminum based cross-linker. Patil et al. (2012) developed a new aluminum based crosslinker that successfully generated a stable gel in temperatures up to 275^{o}F.

Field test of in-situ gelled acids have offered contrasting results. On one hand, Mohamed et al. (1999) has reported irreversible reduction in permeability when in-situ gelled acids were used to stimulate water injector wells in low permeability carbonate

zones. On the other hand, Saxon et al. (2000) and Haldar et al. (2004) have reported effective diversion caused by injection of in-situ gelled acids in highly permeable heterogeneous reservoirs in temperatures up to 120^{o}C.

In recent years, Maheswari et al. (2016) and Hosseinzadeh et al. (2017) have developed a two- scale continuum model which simulates the reactive flow and propagation of wormholes generated by the injection of in-situ gelled acids in single and dual core systems.

The present work examines the viability of a novel cationic polymer based in-situ gelled acid system and endeavors to optimize the said acid system for use as a diversionary agent in carbonate reservoirs.

CHAPTER III

PROBLEM STATEMENT

In-situ gelled acids have been used extensively over the years for the purposes of diversion in heterogeneous carbonate reservoirs. In absence of an appropriate diversion mechanism, the acid flows in the path of least resistance bypassing the lower permeability zones altogether. The increased viscosity of the polymer-based acid system allows the stimulating fluid to contact the low permeability regions of the reservoir. However, there are some major challenges involved in using such a diversion mechanism; primarily the precipitation of polymers and iron based crosslinker which leads to an irreversible reduction in rock permeability (Lynn and Nasr-El-Din 2001, and Taylor and Nasr-El-Din 2003).

The current study attempts to examine the viability of a cationic polymer based in situ gelled acid system. This polymer being primarily cationic is expected to reduce precipitation on the carbonate rock surface which by itself is also cationic. This system has demonstrated a self-breaking ability, which in turn is also expected to minimize the cleaning problem caused by the polymer degradation. The study deals with optimizing the said polymer-acid system for maximum diversion in a heterogeneous carbonate system.

CHAPTER IV

RESEARCH OBJECTIVE

Rheological studies will be conducted on the in-situ gelled acid system to study the viscosity as a function of temperature. The acid will be spent using calcium carbonate to simulate the changes in the viscosity of the system as the acid reacts with the carbonate rock surface. The viscosity of the system will be observed as a function of shear rate at live acid (pH 0) and partially spent acid conditions (pH of 2, 4.5). Changes in the viscoelastic parameters (G', G") of the system will be monitored to see how the viscous behavior changes with pH. Impact of salinity and initial concentration of acid on the viscosity of the system will also be studied.

Single and dual coreflood studies will be conducted in Indiana limestone cores to determine the actual process of diversion and the propagation of the wormhole. The impact of temperature and flow rate will be investigated in both sets of tests. Single coreflood tests will be used to determine how the initial permeability of the core effected the diversion process. Effluents from the single coreflood studies will be studied to determine if any precipitation of iron or polymer took place inside the cores leading to reduction in permeability. Dual coreflood tests will be used to study how permeability contrast impacted the wormhole propagation in both cores.

CHAPTER V

MATERIALS

V.1 Fluids

The formulation of the acid polymer system is listed in **Table 1**. The system contains an acid, a cationic polymer, a cross-linker, and a corrosion inhibitor. ACS grade hydrochloric acid was purchased from Macron Fine chemicals. The polymer and the corrosion inhibitor were supplied by a local chemical company. The polymer is a polyacrylamide made of 90% DMA3Q and 10% acrylamide with an activator package composed of alcohol ethoxylate. $FeCl_3$ was used as a source of Fe^{3+}, which was the crosslinker. ACS grade calcium carbonate powder was used to spend the live acid solutions.

Component	Concentration
Hydrochloric Acid (HCl)	5 wt%
Acid Gelling Agent (Polymer)	2.5 vol%
Corrosion Inhibitor	1 vol%
Cross-Linker: Ferric chloride (40 wt %)	1 vol%

Table 1: Formulation of the in-situ gelled acid

The strength of HCl was determined by titration against a freshly prepared 1.0 N sodium hydroxide solution. The concentration of HCl was found to be 36.8 wt%. Acid solutions were prepared by dilution to 5 wt% with de-ionized water (resistivity 18.2 MΩ at 77^{o}F). 1 vol% corrosion inhibitor was added to avoid any corrosion of the equipment.

This is followed by a gradual addition of the polymer into the fluid system. The crosslinker was added at the end and the solution was mixed for 30 minutes to prevent the formation.

The density for the acid-polymer solution was measured using Anton Paar DMA 4100 density meter and was found to be 1.412 g/cm^3 at 78^{o}F.

V.2 Rock Properties

A total of 11 cylindrical cores were drilled from 4 outcrop Indiana Limestone block for coreflood studies. The dimension of each core was 6 in. length and 1.5 in. diameter. Cores from each block were drilled in one direction to maintain permeability anisotropy. The mineralogy of the Indiana limestone cores was characterized by x-ray diffraction (XRD). Limestone is essentially 99 wt% calcite. **Table 2** shows the mineralogy of the limestone rocks.

Mineral	**Concentration (wt%)**
Calcite	99.86
Dolomite	0.14

Table 2: Mineralogy of Indiana Limestone

CHAPTER VI

RHEOLOGICAL STUDIES

Rheology of the in-situ gelled acids have been proven to have a major impact on the diversion process. The viscosity and the viscoelastic parameters (G', G") of the in-situ gelled acid were characterized in these studies and their changes with variation in the pH of the system monitored. The tests were conducted over a range of temperatures (80, 150, and 250^{o}F). In addition, the impact of salinity and the concentration of the acid on the rheology of the acid system was also investigated. The objective of these tests was to optimize the in-situ gelled acid system to generate maximum diversion in heterogeneous carbonate reservoirs.

VI.1 Experimental Procedure

VI.1.1 Components of Viscometer

Grace M5600 is a HP/HT viscometer and it was used to measure the rheological properties of the live and the partially spent in-situ gelled at a pressure of 400 psi and over a range of temperatures (**Fig. 1**). The viscometer consists of the following components:

1. A rotor and bob system for rotation of the viscous fluid. The bob and rotor were made of Hastelloy C to resist corrosion by the acid.
2. A sample cup, which holds the sample volume while being tested.
3. An oil bath to maintain the desired temperature of the sample.

4. A nitrogen cylinder to apply pressure on the sample and prevent its climbing during the test.
5. Gauges and regulators to control the applied pressure on the sample.
6. A computer with the M5600 software which allowed us to set up, and control the experiments. The data generated from the experiments was later recorded in the software.

Fig. 1: HP/HT Viscometer

VI.1.2 Viscosity and Viscoelastic Parameter Measurement

Before the start of the experiment, the bob and rotor of the viscometer, and the sample cup were cleaned using acetone, and de-ionized water, to ensure no presence of impurities. The required volume of the live acid sample was then added into the sample cup and loaded into the viscometer. Any prior stress in the viscometer was zeroed to remove its impact on the rheological property measurements. The sample cup was subsequently placed in the oil bath. The sample was then pressurized to 400 psi with Nitrogen to prevent the acid from rising during the test. The experimental parameters (temperature, shear rates, frequency) were set using the software. Once the test was completed, the pressure was released. When the system cooled down to room temperature, the sample was released from the viscometer. The sample cup was removed from the viscometer and the entire viscometer was cleaned thoroughly with acetone and water.

These tests were repeated with the partially spent in-situ gelled acids over a range of pH values. The spending of the live acid was carried out by gradually adding calcium carbonate powder to the system. The addition of calcium carbonate is meant to simulate the reaction that would occur on the carbonate rock surface with the acid. The pH of the system is monitored using an Oakton pH meter.

VI.2 Results and Discussion

The polymer- acid system exhibited a non-Newtonian shear thinning behavior. The relationship between viscosity and shear rate was described by the power-law model, **Eq. 1**:

$$\mu = K.\gamma^{n-1} \quad (1)$$

Where μ is the fluid viscosity, cp; K is the power-law constant, cp.s^n; γ is the shear rate, s^{-1}; and n is the power-law index.

The viscosity of the live acid system (pH 0) was measured as a function of shear rate from 0 to 1,000 s^{-1}.

VI.2.1Acid Spending Experiments

The acid system showed a dramatic increase in viscosity once the pH reached 2 (**Fig. 2**). The viscosity of the system increased from 109.08 cp for the live acid to 653.1 cp for pH 2 at 10 s^{-1} and 150^{o}F. The viscosity kept increasing with the increase in the pH, until it reached 4.5 with the maximum reported viscosity of 934 cp. Subsequently, the gel broke down and the viscosity of the system declined significantly to 209.46 cp. The rheological parameters of the in-situ gelled acid system are listed in **Table 3**. Similarly, for 250^{o}F (**Fig.3**), the viscosity of live acid at 10 s^{-1} increased from 117 cp to 185.8 cp for pH 2. The maximum viscosity reported was 265.7 cp. The viscosity of the system declined to 69.1 cp with the breakdown of gel after it reached a pH of 4.5. The rheological parameters are listed in **Table 4**.

The results indicate that the polymer is cross-linked by the ferric ions once the pH of the system was 2. The site for crosslinking is expected to be the lone pair of electrons on the double bonded oxygen atom on the DMA3Q. The increased viscosity of the acid will block the high permeability zone, and force the subsequent acid of lower viscosity to be diverted to untreated zones. Once the pH increases to value above 4.5, the ferric ions reduce to ferrous which can no longer crosslink the polymer and the gel breaks down (Hill 2005).

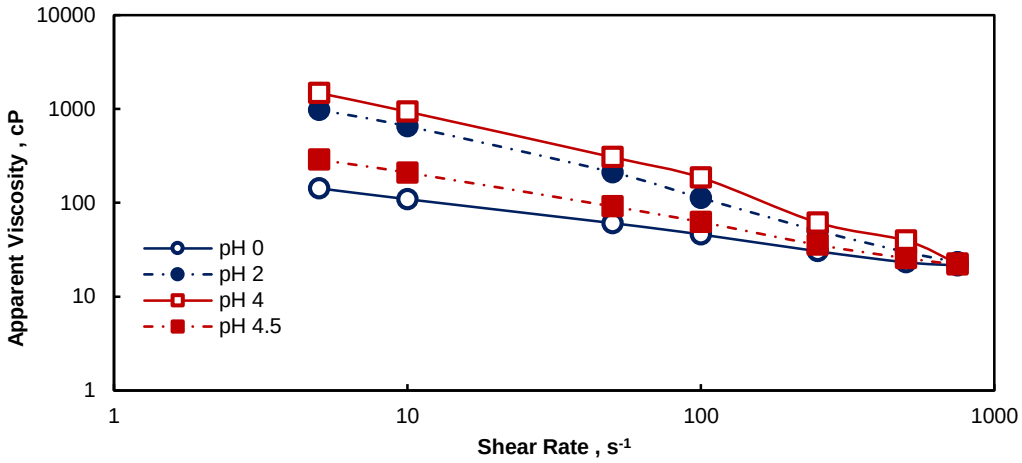

Fig. 2: Viscosity of the live and partially spent acid as a function of shear rates at 150°F.

Acid concentration	K (cp.s^n)	n	R^2
pH 0	267.68	0.613	0.9982
pH 2	3703	0.233	0.9972
pH 4	6499	0.173	0.989
pH 4.5	690.4	0.474	0.9987

Table 3: Rheological properties of the live and partially spent acid as a function of shear rates at 150°F.

This observation is further supported by the frequency sweep experiments conducted on the live and partially spent acid (**Fig. 4 & 5**). The G', G" measurements indicated that the live acid exhibited weak viscoelastic properties with a G' value of 0.767 Pa at 1 s^{-1} and G" value of 0.63 Pa at 1s^{-1} at 80°F. After the polymer crosslinks at pH 2, the viscoelastic parameters improve significantly. The elastic modulus (G') increases to 5.177 Pa at 1s^{-1} while the viscous modulus (G") increases to 1.876 Pa. The dramatic increase in the G' value as compared to the G" indicated that after the pH of 2, the in-situ gelled acid behaved as a semi-solid elastic gel which would force the following acid to flow into the next higher permeability zones.

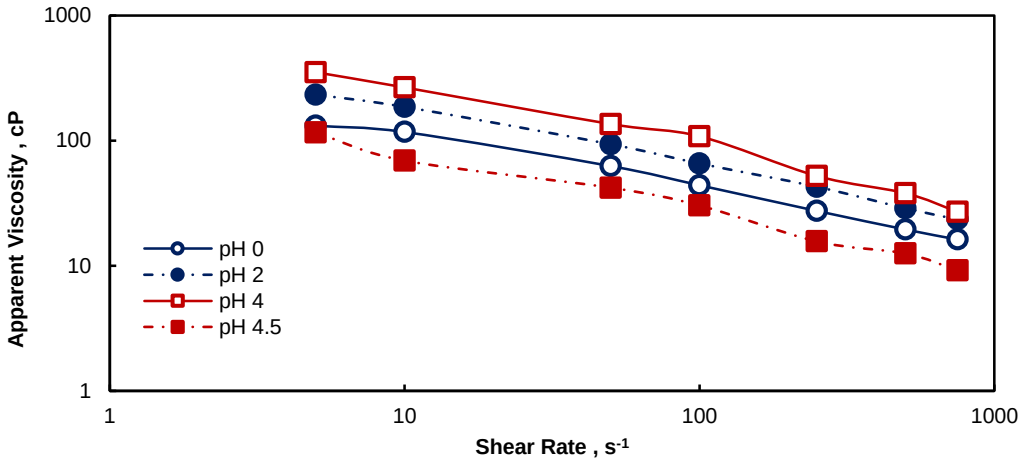

Fig. 3: Viscosity of the live and partially spent acid as a function of shear rates at 250°F.

Acid concentration	K (cp.s^n)	n	R^2
pH 0	301.3	0.567	0.989
pH 2	529.4	0.537	0.9958
pH 4	881.9	0.505	0.983
pH 4.5	246.3	0.515	0.9859

Table 4: Rheological properties of the live and partially spent acid as a function of shear rates at 250°F.

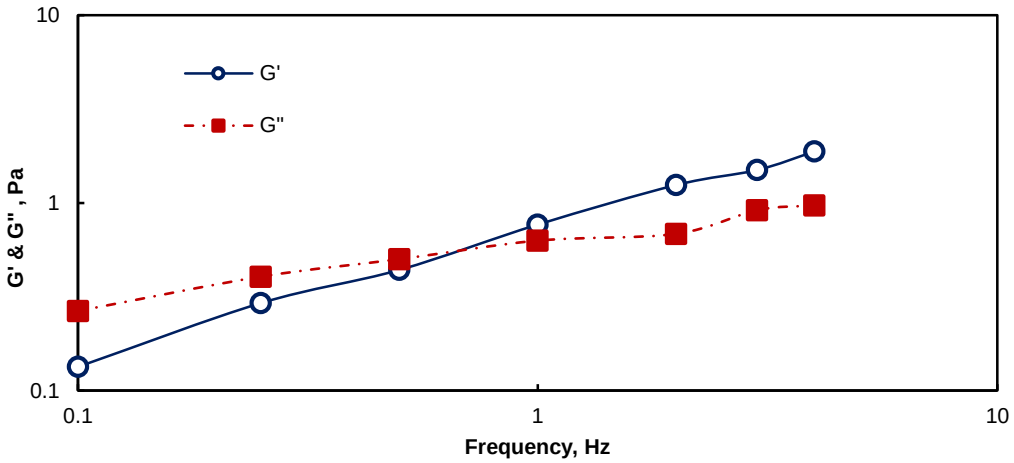

Fig. 4: G', G" of the live acid at 80°F.

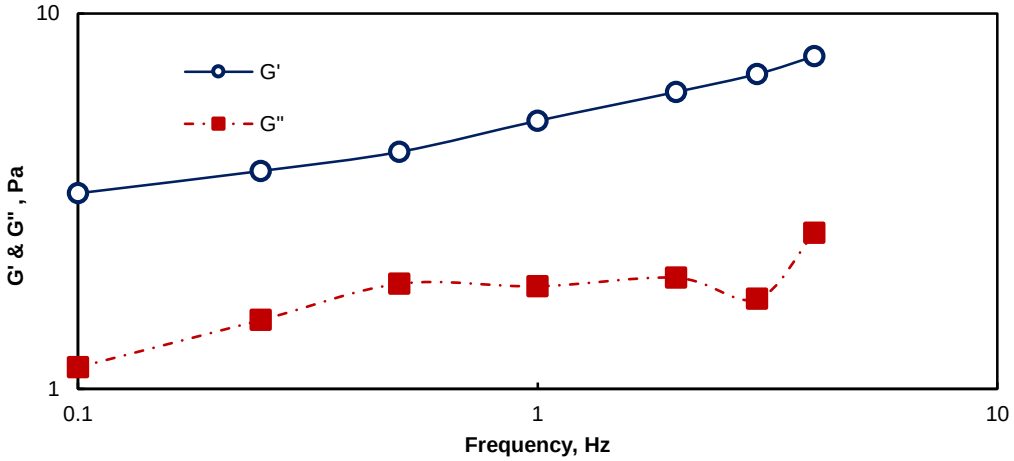

Fig. 5: G', G" of the partially spent acid (pH 4) at 80°F.

VI.2.2 Salinity

The in-situ gelled acid systems were prepared with DI water and 5 wt% KCl to determine the impact of salts on the viscosity of the live and partially spent systems. It was observed that the addition of salts to the system lead to a decline in the viscosity of the live acid (**Fig. 6**) over the entire range of shear rates measured. The rheological properties of the two acid systems are tabulated in **Table 5**. When the acids were spent with calcium carbonate, the viscosity of the KCl system was lower than the system with DI water for the entire range of equilibrium pH measurements (**Fig. 7**).This decline in viscosity can be explained by the fact that the salts affected the configuration of the polymer, causing the polymer to separate out of the solution.

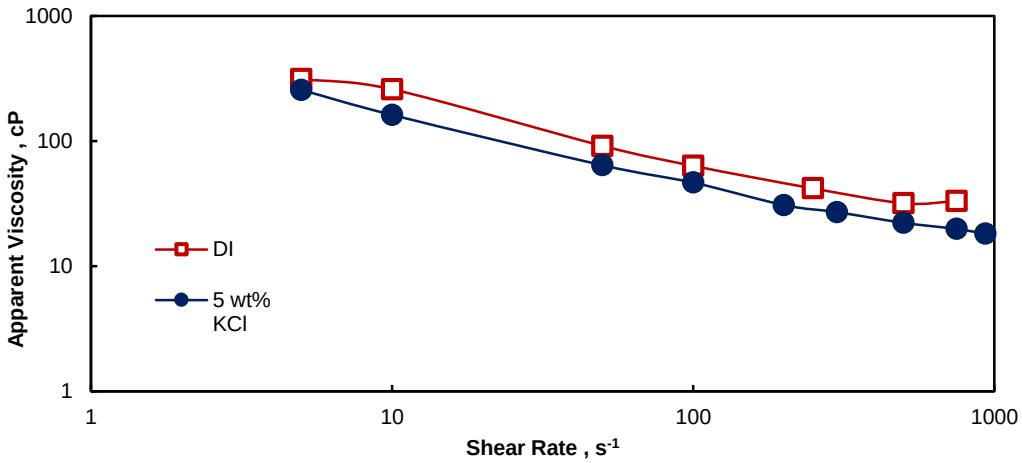

Fig. 6: Viscosity of the live acid prepared with DI water and 5 wt% KCl as a function of shear rates at 80°F.

Acid concentration	K (cp.s^n)	n	R^2
DI water	686.01	0.511	0.9807
5 wt % KCl	511.15	0.494	0.9897

Table 5 : Rheological properties of the live acid prepared with DI water and 5wt% KCl as a function of shear rate at 80°F.

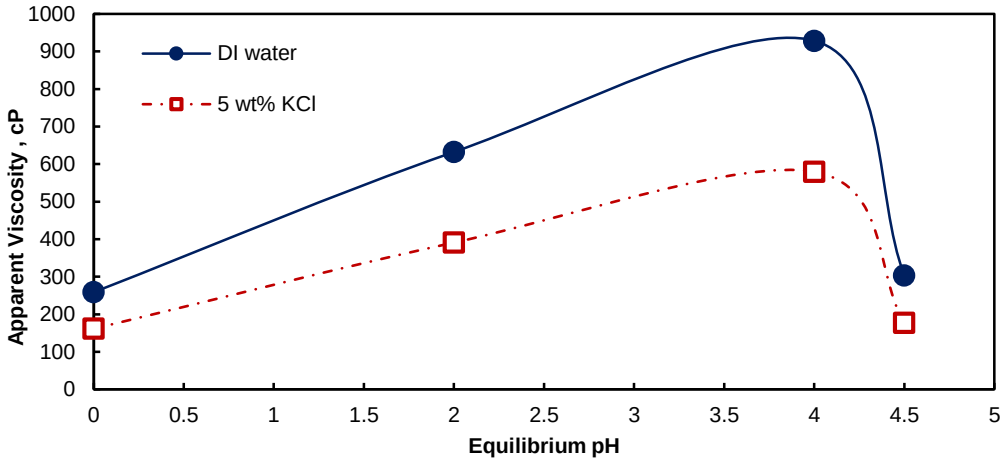

Fig. 7: Viscosity of the acid prepared with DI water and 5wt % KCl as a function of equilibrium pH at 80°F and 10 s^{-1}.

VI.2.3 Live Acid Concentration

The acid system was prepared at three different concentrations of HCl: 3, 5, and 15 wt%. The viscosities of these 3 acid systems were measured at 80°F. It was observed that an increase in the acid concentration lead to a decrease in the viscosity of the system across the range of shear rates (**Fig. 8**). The decrease in viscosity was much more apparent when the acid concentration was decreased from 5 to 15 wt% HCl acid solution as compared to when the acid concentration decreased from 5 to 3 wt%. Gomaa and Nasr-El-Din (2010 c) noted that the higher concentration of acid will lead to a greater release

of calcium ions on reaction with calcium carbonate. The increased calcium ions cause a decline in the viscosity of the of the spent in-situ gelled acid. This was also observed when all the three live acids were spent to equilibrium pH values of 2, 4, and 4.5 and their viscosity was recorded at a shear rate of 10 s^{-1} (**Fig. 9**). Thus, a 5 wt % HCl concentration is recommended as higher acid concentration does not generate a higher viscosity needed for diversion. The rheological parameters of the in-situ gelled acid systems are listed in **Table 6**.

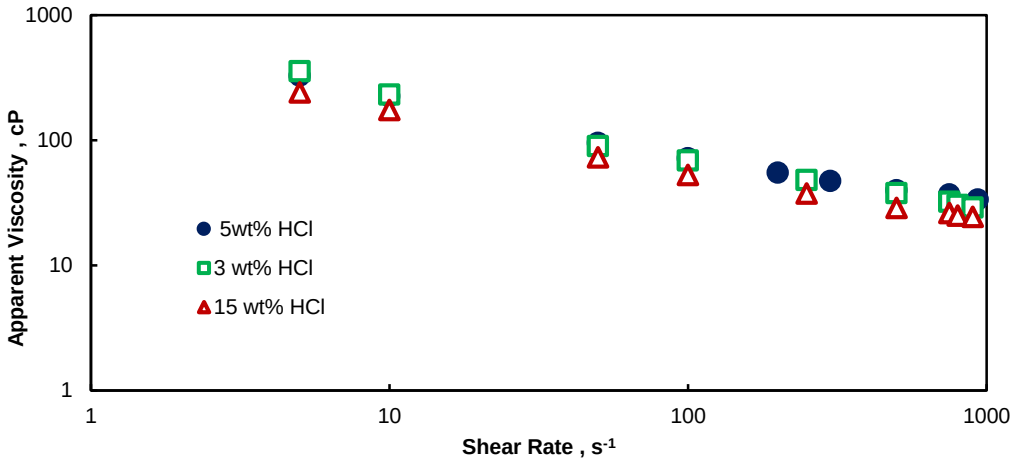

Fig. 8: Viscosity of the live acid prepared with 3,5, and 15 wt% HCl as a function of shear rate at 80°F.

Acid concentration	K (cp.s^n)	n	R^2
3	660.7	0.534	0.9891
5	585.5	0.567	0.9869
15	452.84	0.56	0.9915

Table 6: Rheological properties of the live acid prepared with 3,5, and 15 wt% HCl as a function of shear rate at 80°F.

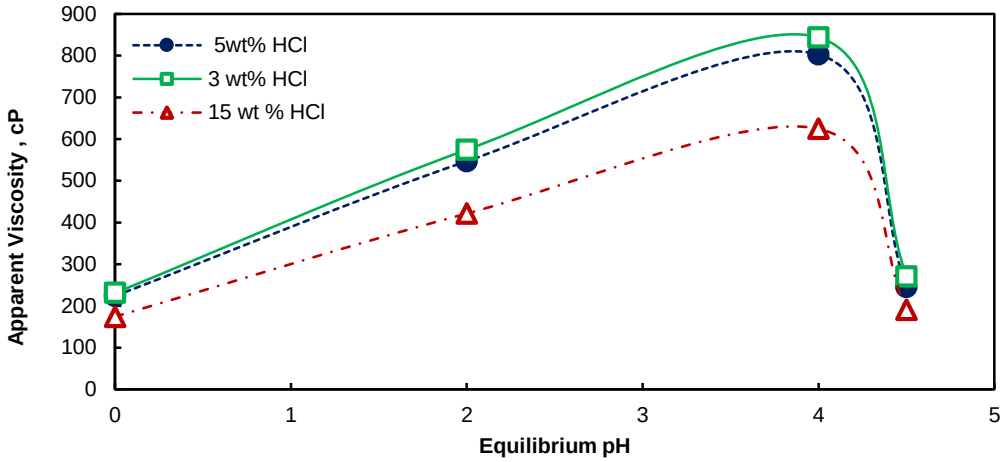

Fig. 9: Viscosity of the acid prepared with 3,5, and 15 wt% HCl as a function of equilibrium pH at 80°F and 10 s^{-1}.

CHAPTER VII

COREFLOOD STUDIES

The diversion characteristics of the in-situ gelled acid system was investigated by conducting coreflood tests with Indiana limestone cores. Two different types of coreflood tests were conducted: single and dual coreflood. The objective of the single coreflood tests was to characterize the wormhole generated by the in-situ gelled acid system and to investigate if there was any damage caused by the system. The impacts of flow rate, initial permeability of the zone, and temperature on the generation and propagation of wormhole were studied. The tests were conducted over three different injection rates and over a range of three temperatures (80, 150, and 250^{o}F). The objective of the dual coreflood tests were to study how permeability contrast impacts the ability of the in-situ gelled acids to cause diversion. In addition, the impact of flow rate, and temperature on the process of diversion was also investigated.

VII.1 Experimental Procedure

VII.1.1 Components of Coreflood

The schematic diagram of the coreflood apparatus is shown in **Fig 10.** The apparatus consists of the following components:

1. An ISCO syringe pump that injects fluids into the core at a constant flow rate or constant pressure.
2. Two accumulators for the acid and the deionized water.

3. A 6 in. stainless steel core holder with a rubber sleeve; two 6 in. core holders for dual coreflood experiments.
4. An electric oven which houses the core holders and maintains the required temperature.
5. A hydraulic pump that applied overburden pressure on the core. Hydraulic oil was injected into the annular space between the core holder and the rubber sleeve and pressurized to simulate the pressure applied by the overburden layers of the rocks in a conventional reservoir.
6. Gauges and regulators to monitor and control the pressure drop across the core over time.
7. A nitrogen cylinder to apply back pressure to prevent gases such as CO_2 to evolve out of the solution inside the core and interfere with the reaction.
8. A pressure transducer to measure the pressure drop across the core. The pressure transducer was connected to the data acquisition system (LABVIEW) to record the pressure drop across the core during the progress of the experiment.

VII.1.2 Core Preparation

Cores were drilled from Indiana limestone block with a diameter of 1.5 in. and length 6 in. The cores were dried overnight in an oven at 250^{o}F followed by complete saturation with deionized water under vacuum for 6 hours. The pore volume and the porosity were calculated by the weight difference method (**Eq. 2 and 3**).

$$PV = \frac{W_{sat} - W_{dry}}{\rho} \quad (2)$$

$$\phi = \frac{PV}{V_{bulk}} \times 100 \quad (3)$$

where PV is the pore volume of the cores in cm^3; W_{sat} and W_{dry} are the saturated and dry weights of the core in g; ρ is the density of de-ionized water in g/cm^3; ϕ is the porosity of the core in vol %; V_{bulk} is the volume of the core in cm^3.

VII.1.3 Coreflood Experiments

The deionized water saturated core was loaded into the core holder, and a back pressure of 1,100 psi was applied to ensure that most of the CO_2 evolved during the reaction of the acid with the rock is kept in solution. An overburden pressure of 1,800 psi was applied to ensure that the fluids did not bypass the core.

Initially, the permeabilities of the cores were determined by injecting de-ionized water at injection rates of 2,4, and 6 cm^3/min at room temperature, using Darcy's equation (**Eq. 4**).

$$k = \frac{Q \times \mu \times Lo}{A \times \Delta P} \quad (4)$$

where k is the absolute permeability in Darcy; Q is the flow rate in cm^3/min; μ is the fluid viscosity in cP; L_0 is the length of the core in cm; A is the cross section of the core in cm^2; and ΔP is the pressure drop across the core in atm.

The porosities and permeabilities of all the cores used in coreflood studies are given in **Table 7**. Once these parameters were determined, the cores were heated to the specified temperature with a continuous injection of DI water until a stable pressure drop across the cores was observed. For the single coreflood system, this was followed by the injection of acid solution until breakthrough was achieved which was marked by a significant pressure drop. After breakthrough was observed, DI water was injected till a clear effluent sample was collected. For the dual coreflood system, 1 PV of in-situ gelled acid was first injected which was then followed by 1 PV of 15 wt% HCl. Subsequently, DI water was injected until the pressure drop across both the cores stabilized.

Core effluent samples were collected every 0.5 PV and their pH was measured using Oakton pH meter. They were further diluted to be analyzed for calcium and iron ion concentration by Inductively Coupled Plasma Optical Emission Spectroscopy (ICP-OES) analysis by Perkin Elmer using Optima 7000 DV ICP-OES system and WinLab 32^{TM} software. The acid concentrations in the core effluent samples were measured by titration against 0.1M NaOH solutions in a Metrohm 907 Titrando auto-titrator and were reported in terms of equivalent HCl. The effluent samples collected during the dual coreflood experiments were studied for the change in the flow rate of volume collection. The cores were scanned by X-ray computed tomography (CT), and the images for wormhole structures were generated using Osirix software.

Experiment set	Core ID	Acid injection rate, cm^3/min	PV, cm^3	Temperature, ^oF	Porosity, vol%	Absolute permeability(k), md
Single coreflood	116	7.5	25	150	14.39	103.1
	117	2.5	24.3	150	13.99	98.6
	118	5	24.8	150	14.28	89.9
	119	5	22.8	150	13.13	9.89
	104	5	24.4	250	14.05	113.2
Dual coreflood	128 111	5	25.2 22.7	150	14.5 13.07	63.2 7.19
	125 131	5	25.5 22.9	150	14.68 13.18	58.9 19.7
	133 139	5	25.8 24.7	150	14.85 14.22	103.6 22.5

Table 7: Porosities and permeabilities of cores used in coreflood experiments.

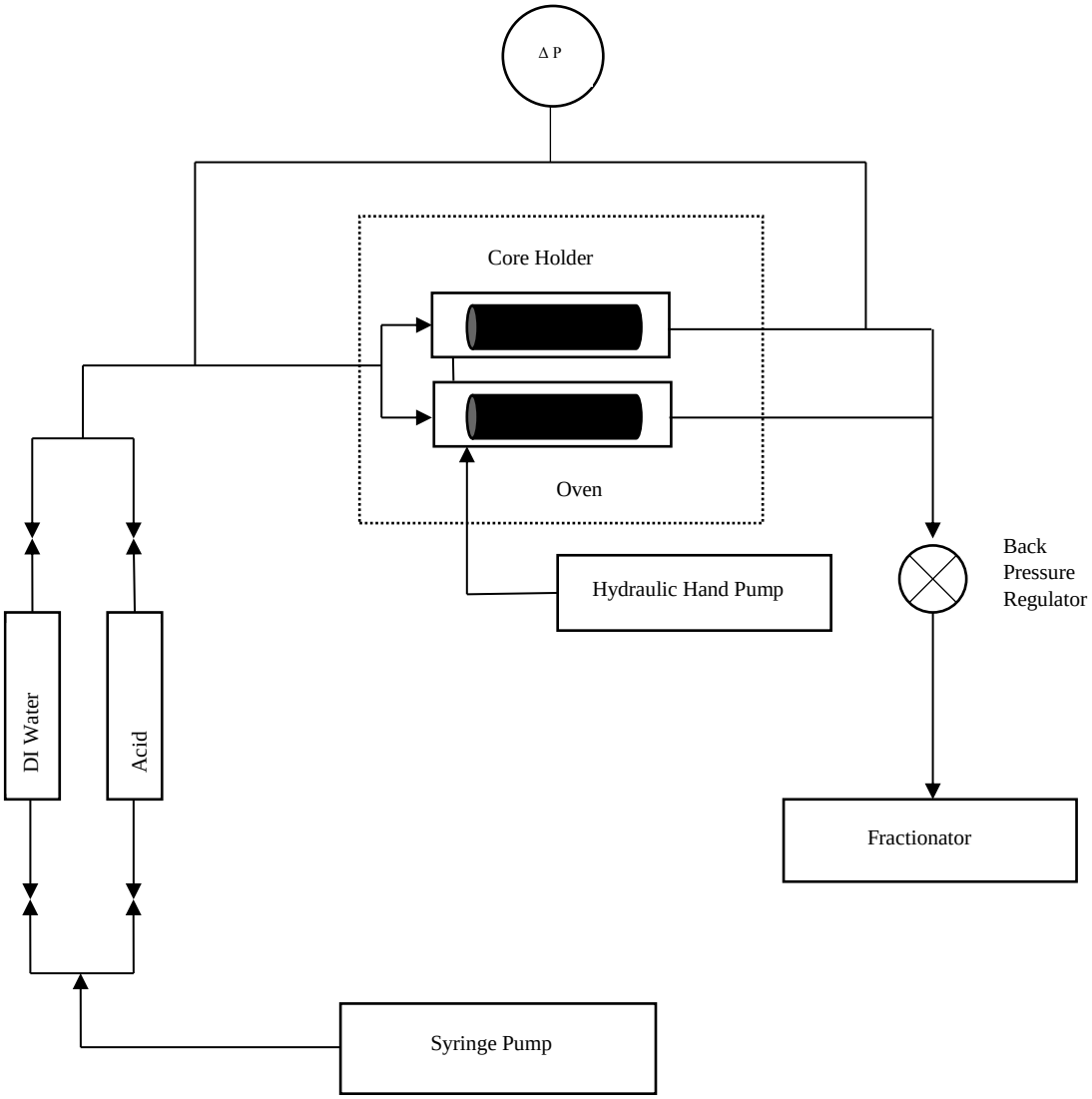

Fig. 10: A schematic of coreflood set-up

VII.2 Theory of Wormhole Formation

Wormholes are highly conductive channels generated when reactive fluids, like acids, are injected into a porous media causing the dissolution of minerals. These wormholes provide a low resistance path for fluid flow after stimulation is done. When acid is injected into the core, some acid advances ahead of the initial reaction front and

dissolves the mineral (Hoefner and Fogler 1988). In a conventional acid system, this leads to a lower resistance for the acid to flowing behind the initial front and leads to more dissolution behind the front, as compared to the advancing tip of the wormhole. This causes fluid from other region to divert into this channel because of the lower resistance to flow in the wormhole.

However, in an in-situ gelled acid system, the fluid at the wormhole tip increases in viscosity when it spends beyond a pH of 2 while progressing into the core. The gel is formed when the crosslinking of the acid system occurs and it plugs the wormhole. This would force the live acid that is behind the wormhole tip to be pressurized because of the constant injection rate. The pressure continues to increases until the acid breaks through the weakest point in the core (typically the next highest permeability zone) and changes its direction.

There are two resistances that determine the structure of the wormhole: transport of acid and the reaction products (mass transfer) and the actual reaction of acid on the rock (surface reaction limited kinetics.) If the reaction between the rock and the acid occurs faster than the diffusion of acid, the reaction is termed mass transfer limited. On the other hand, if the transport of the reactive fluid occurs faster than the reaction at the surface, the reaction is deemed as surface reaction limited. Rabie et al. (2011) reported that for an in-situ gelled acid system, the reaction with calcite is mass-transfer limited up to rotational speed of 1,000 rev/min and is surface reaction limited above this at 150^{o}F.

VII.3 Single Coreflood Studies

The objective of the single coreflood studies were to examine the wormhole generated by the in-situ gelled acid in a carbonate environment. The possibility of polymer and iron precipitation during the injection of the acid was also investigated. The impact of flowrate, initial core permeability, and temperature on the generation of wormholes were studied. A total of 5 single corefloods were conducted.

VII.3.1 Impact of Flowrate

Three coreflood experiments were performed at injection rates of 2.5, 5, and 7.5 cm^3/min. These tests were conducted at 150^oF.

At Injection Rate 2.5 cm^3/min

3.15 PV of acid was injected before breakthrough occurred. The CT scan image of the core showed face dissolution with a larger diameter wormhole at the inlet face, which tapered as it approached the outlet (**Fig. 11**). The arrow indicates the direction of the wormhole growth. The low flow rate of 2.5 cm^3/min caused the acid system to have a long residence time in the core leading to the consumption of excess acid at the core entrance. Despite the lowered reactivity of the acid system caused by its increased viscosity, the dissolution reaction is still faster than the acid transport rate and it causes a greater volume of acid consumption on the wormhole walls close to the core inlet (Hoefner and Fogler 1988; Bazin 2001). The wormhole displayed significant tortuosity.

There was an increase in the pressure drop when the acid reached the inlet face of the core (**Fig. 12**). This is because of the higher viscosity of the acid system as compared to the preflush DI water and one of the reaction products that evolved when the acid comes in contact with the core, gaseous CO_2 is not completely dissolved in the fluid stream. The pressure drop continued to increase with a constant cyclical oscillation till it reaches a maximum just before breakthrough. The oscillatory nature of the pressure drop is due to the continuous change in the direction of the acid which was caused by the gel formed by the partially spent acid plugging the core.

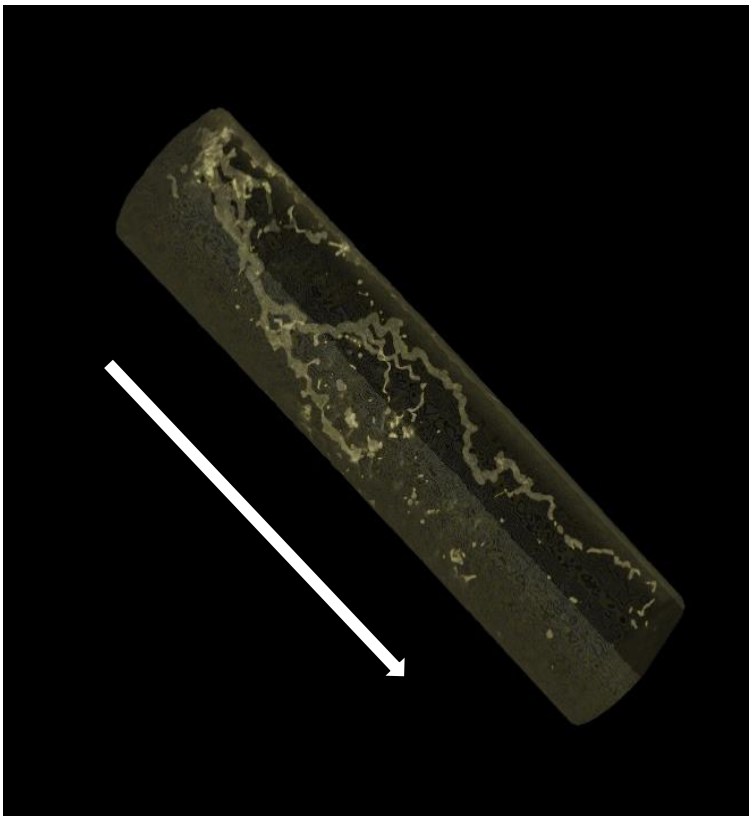

Fig. 11: CT scan image of Indiana limestone after acidizing at 2.5 cm^3/min.

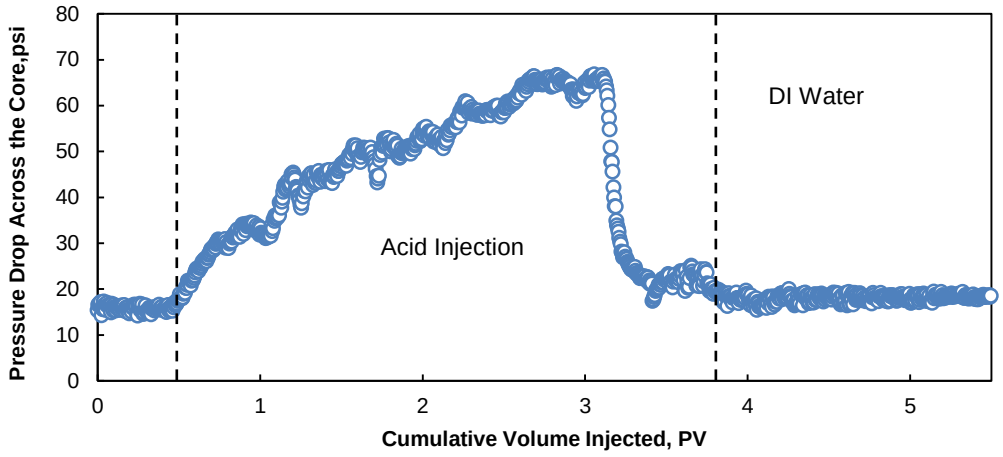

Fig. 12: Pressure drop across the core for the acid injection at 2.5 cm^3/min as a function of the cumulative volume injected at 150°F.

Maximum calcium ions dissolved was about 57,000 mg/L and the maximum iron concentration was around 1,100 mg/L. (**Fig. 13**). Material balance studies were conducted by measuring the total amount of iron recovered in the effluent samples by measuring the area under the iron concentration curve and comparing it with the amount of iron pumped into the core as a crosslinker with the acid. It was found that there was a recovery of 91.8% of the iron in the effluent sample. The rest is assumed to be precipitated on the inlet face of the core. The maximum unconsumed acid concentration at breakthrough, measured in the effluent samples, was around 1.64 wt% equivalent HCl (**Fig. 14**). This proved that a significant acid volume was consumed on the inlet face of the wormhole leaving insufficient volume for further diversion in to the core.

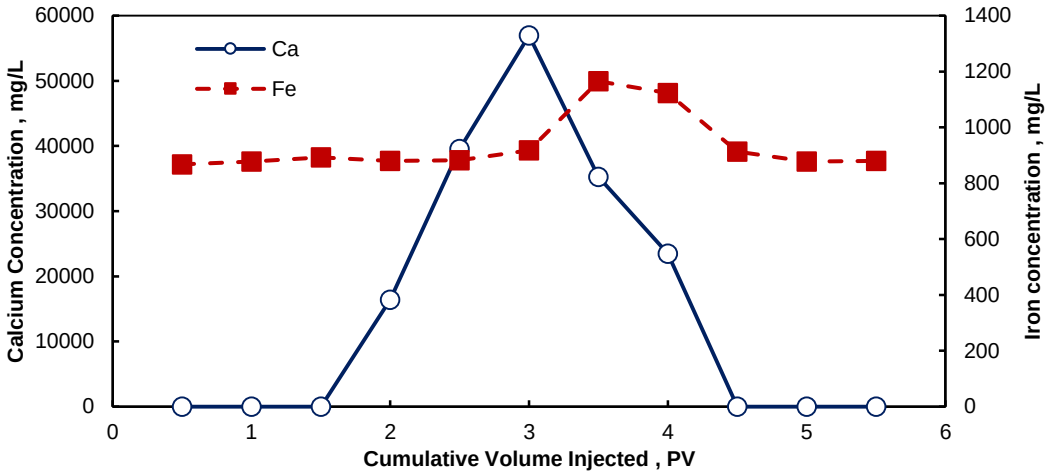

Fig. 13: Calcium and Iron ion concentration for the acid injection at 2.5 cm^3/min as a function of the cumulative volume injected at 150°F.

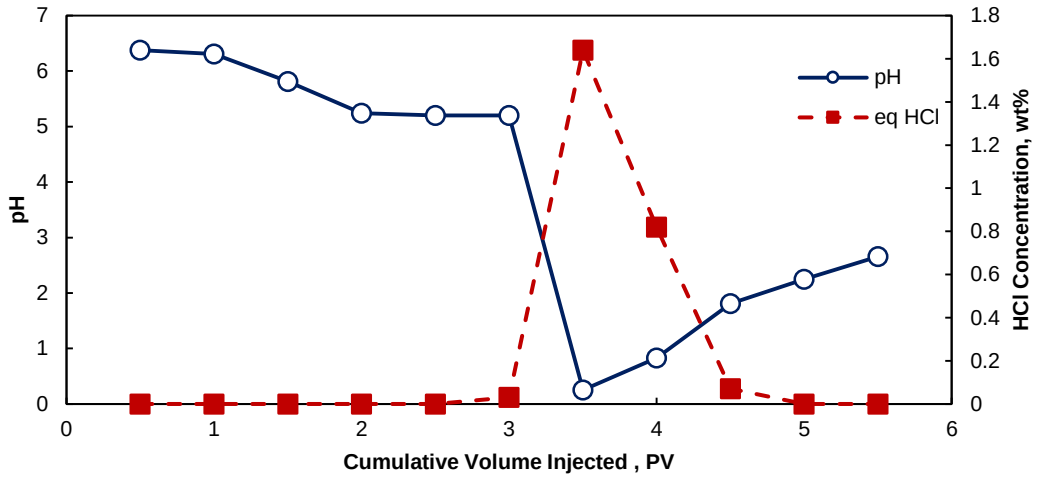

Fig. 14: Acid concentration in terms of equivalent HCl and pH of core effluent samples for the acid injection at 2.5 cm^3/min as a function of the cumulative volume injected at 150°F.

At Injection Rate 5 cm^3/min

3.1 PV of the acid was injected before breakthrough occurred, which was almost similar to that at 2.5 cm^3/min. There was an immediate sharp increase in the pressure drop when the acid reached the core inlet (**Fig. 15**). This indicated that the in-situ gelled acid generated a gel of sufficiently high viscoelastic strength which caused the pressure to shoot up and force the acid from the high permeability region near the inlet face to the next higher permeability zone. The immediate drop in pressure after the initial pressure shoot up provides evidence of this diversion, which can also be seen in the CT scan in the form of a secondary wormhole (**Fig. 16**).

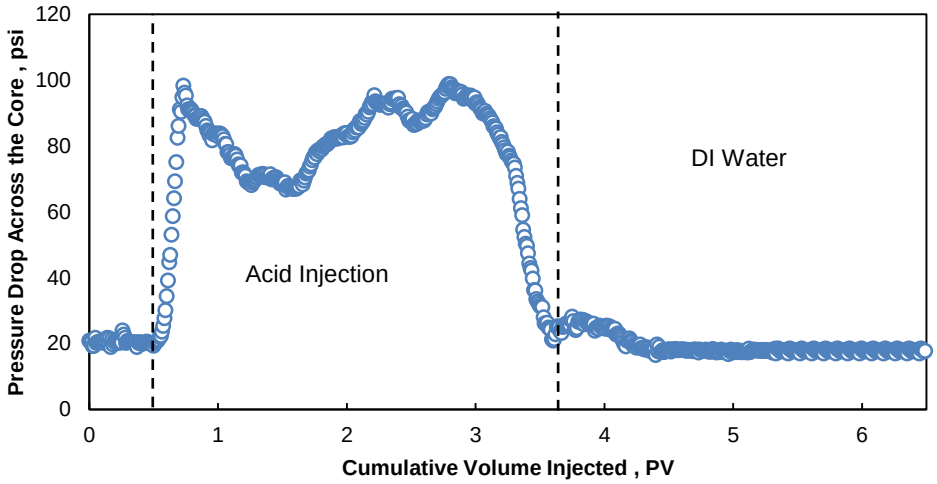

Fig. 15: Pressure drop across the core for the acid injection at 5 cm^3/min as a function of the cumulative volume injected at 150°F.

Because of the higher flow rate, the acid had a lower residence time in the core and thus no dissolution of the inlet face was observed here. The lower consumption of acid in the inlet face led to a higher unspent acid concentration at breakthrough of 2.35

wt% equivalent HCl (**Fig. 17**) as compared to the 2.5 cm^3/min experiment. There was more live acid left at the end of the experiment to propagate the wormhole deeper into the formation and divert more acid into the lower permeability regions of the formation. Maximum calcium ions dissolved was close to 25,000 mg/L (**Fig.**). The percentage of iron recovered in the effluent samples was found to be 91.1% from the material balance studies.

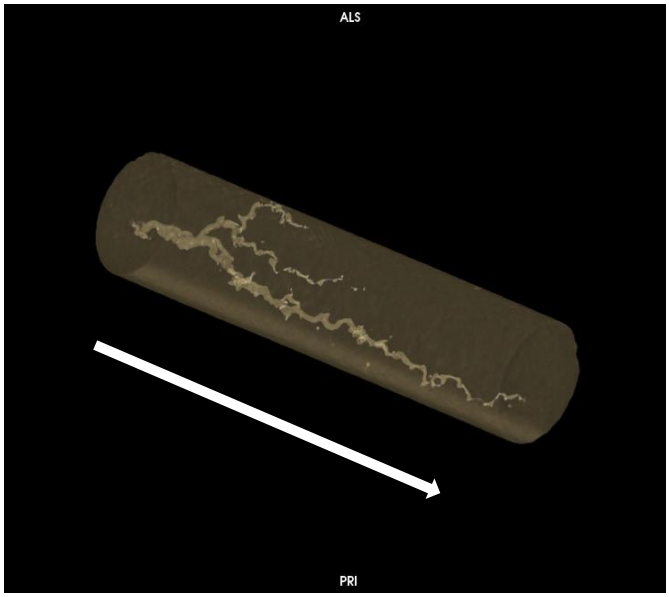

Fig. 16: CT scan image of Indiana limestone after acidizing at 5 cm^3/min.

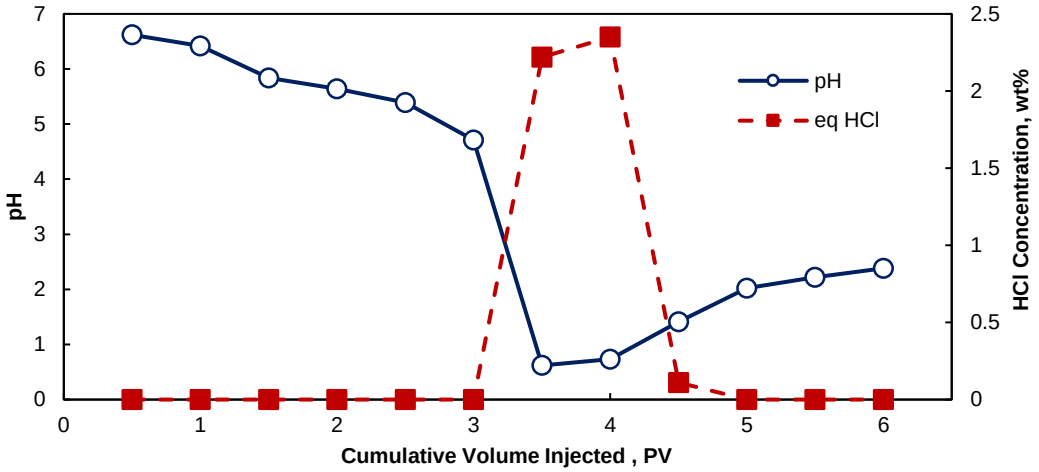

Fig. 17: Acid concentration in terms of equivalent HCl and pH of core effluent samples for the acid injection at 5 cm^3/min as a function of the cumulative volume injected at 150°F.

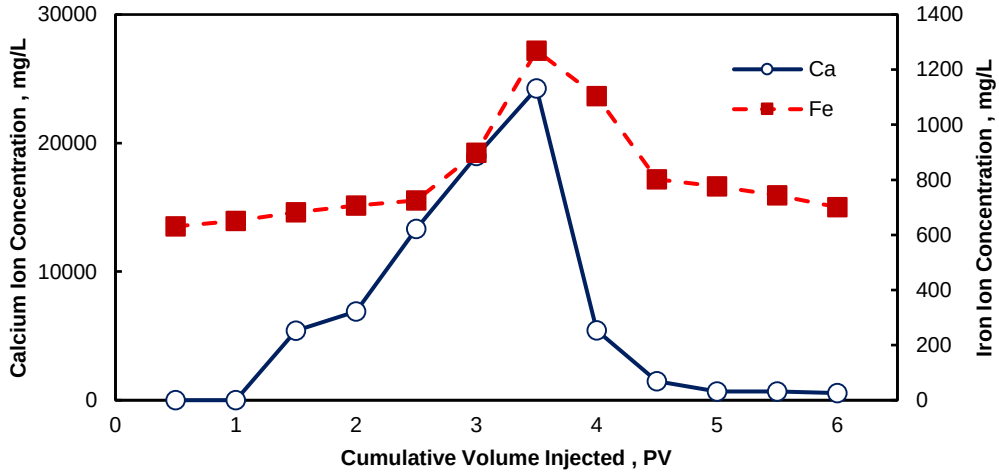

Fig. 18: Calcium and Iron ion concentration for the acid injection at 2.5 cm^3/min as a function of the cumulative volume injected at 150°F.

At Injection Rate 7.5 cm^3/min

3.26 PV of acid was injected before breakthrough occurred, which was significantly higher than that of the previous injection rates. This is because the high shear rate of the injection caused a lower apparent viscosity of the acid system, causing an easier transport of the acid and the reaction products. This facilitated a greater reaction at the rock surface. The pressure drop showed an immediate increase when the acid reached the inlet of the core (**Fig. 19**). Numerous cyclical oscillations of the pressure drop were observed. However, the amplitudes of such pressure drops were very small which indicated that the gel formed on the spending of the acid did not have sufficient viscoelastic strength to successfully divert the acid inside the core.

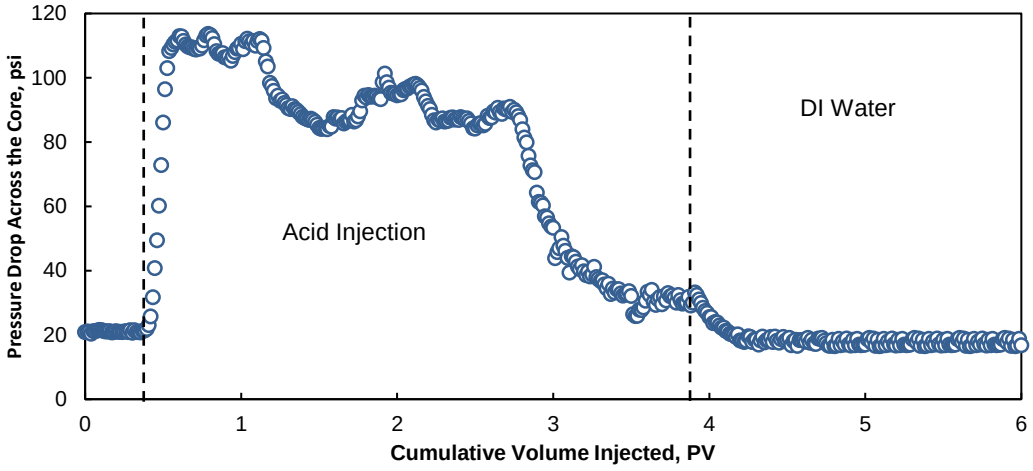

Fig. 19: Pressure drop across the core for the acid injection at 7.5 cm^3/min as a function of the cumulative volume injected at 150°F.

CT scan images indicated that the wormhole generated that was significantly less tortuous (**Fig. 20**). Maximum calcium ions dissolved was about 48,000 mg/L and maximum iron recovered in the samples was 1,200 mg/L (**Fig. 21**). The lower dissolution

of the calcium ions was because of the higher flow rate leading to a lower residence time of the acid inside the core, ultimately leading to lower reaction of the acid inside the core. Percentage recovery of iron in the effluents from the material balance study was found to be 89.2%. The rest is again expected to be precipitated on the inlet face of the core. Maximum unconsumed acid concentration in the effluent samples at breakthrough was 1.61 % equivalent HCl (**Fig. 22**).

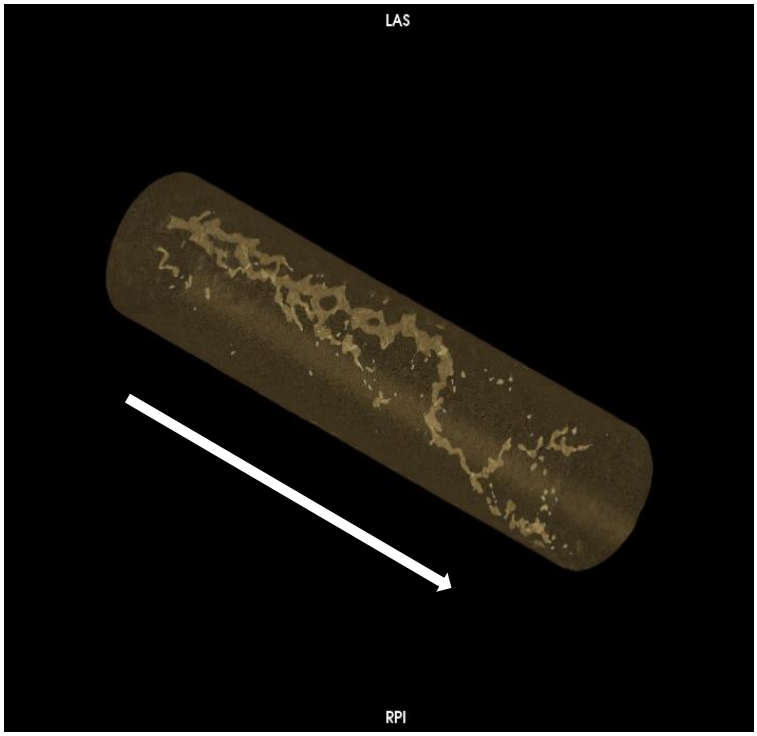

Fig. 20: CT scan image of Indiana limestone after acidizing at 7.5 cm^3/min.

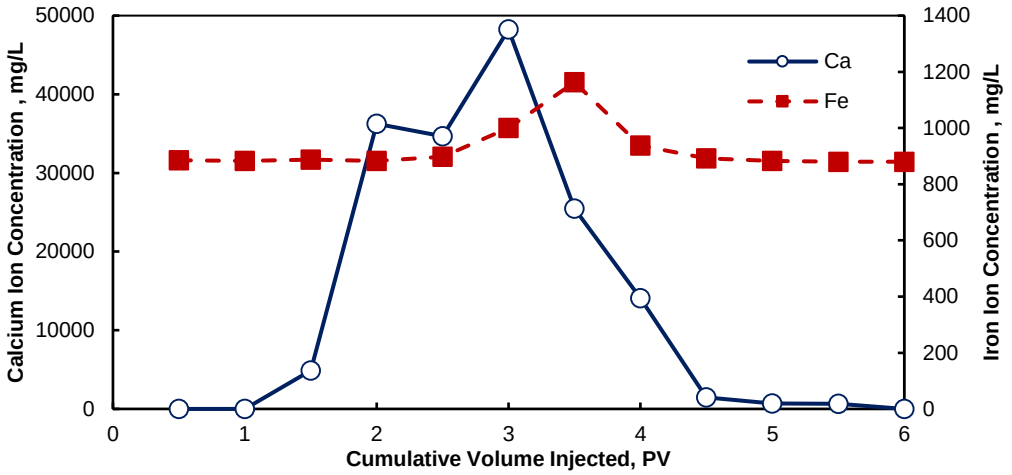

Fig. 21: Calcium and Iron ion concentration for the acid injection at 7.5 cm^3/min as a function of the cumulative volume injected at 150°F.

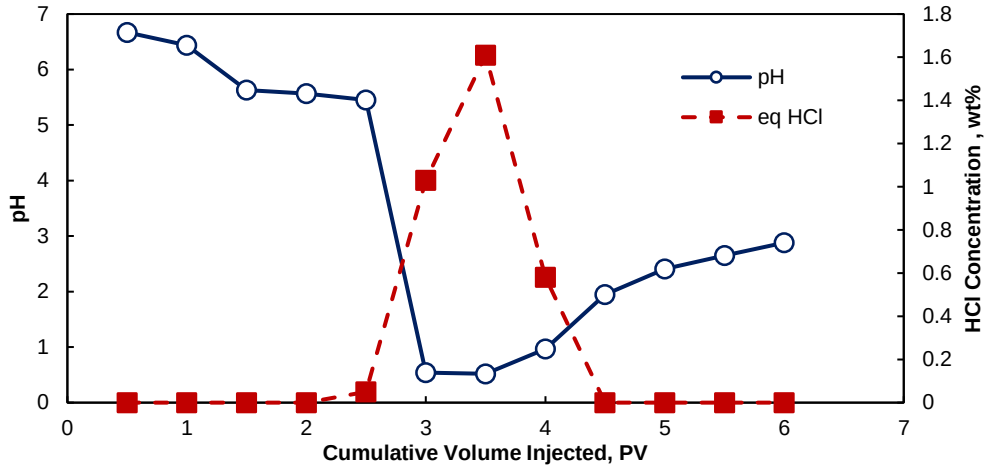

Fig. 22: Acid concentration in terms of equivalent HCl and pH of core effluent samples for the acid injection at 7.5 cm^3/min as a function of the cumulative volume injected at 150°F.

Optimum Injection Rate

The optimum injection flow rate at which the lowest PV (3.1 PV) of the in-situ gelled acid was required for breakthrough was obtained at 5 cm^3/min. At lower flow rates of 2.5 cm^3/min, there was a large consumption of the acid (3.15 PV) in the inlet face because of the longer acid residence time leading to face dissolution of the core. The unreacted acid concentration at breakthrough was 1.64 wt % equivalent HCl. At higher flow rate of 7.5 cm^3/min, the viscosity of the acid lowered significantly to facilitate easier transport of the acid and reaction products. This leads to a greater reaction of the acid inside the rock and ultimately more consumption of acid (3.26 PV). The unreacted acid concentration at breakthrough was 1.61 wt % equivalent HCl. The optimum flow rate of 5 cm^3/min had an unreacted acid concentration of 2.35 wt % of equivalent HCl at breakthrough. **Fig. 23** shows the acid efficiency curve for the injection of the in-situ gelled acid. Thus, 5 cm^3/min injection was chosen as the optimal injection rate and subsequently repeated for all further coreflood studies.

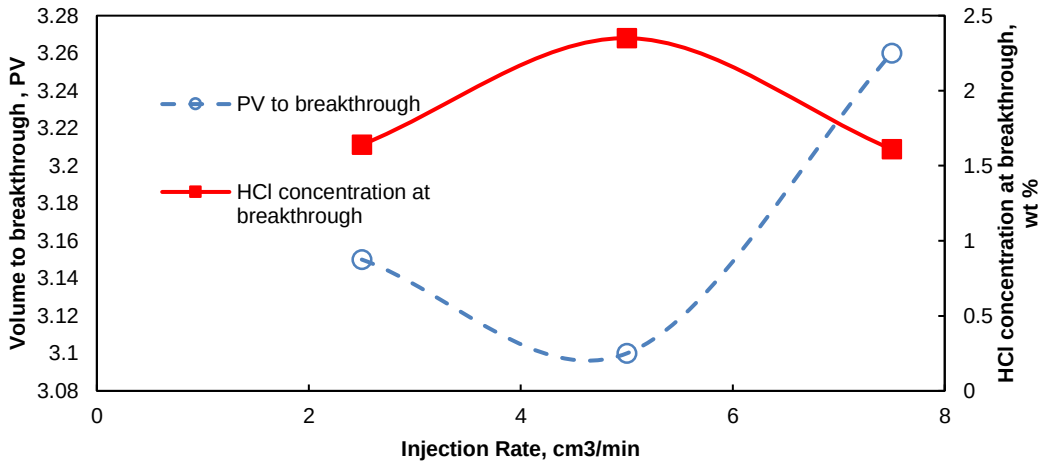

Fig. 23: Acid efficiency curve for the acid at 150°F.

VII.3.2 Impact of Initial Core Permeability

Core permeability plays an important role in the process of diversion, particularly for polymer- based acid systems. This is because the size of the polymer is often larger than the pore throat sizes, which causes the polymer to filter out and precipitate. Thus, coreflood studies were conducted on progressively lower permeability Indiana limestone cores so we could determine if this system would cause any damage due to polymer precipitation. These tests were conducted at the optimal flow rate of 5 cm^3/min and 150^oF.

Initial Core Permeability ~ 10 mD

The PV of blend required to breakthrough at 5 cm^3/min was 2.5 PV. The pressure drop exhibited a large increase immediately when the acid comes in contact with the core (**Fig. 24**). The larger magnitude of the pressure drop is expected to be because of the smaller pore throat size of the lower permeability cores causing a greater resistance to flow of the in-situ gelled acid. A few oscillations of the pressure drop was observed which indicated that there was a change in the direction of flow of the acid inside the core, and it was observed in the CT scan image (**Fig. 25**).

Maximum calcium ion dissolved was around 30,000 mg/L while the maximum iron recovered in the effluent sample was 1,000 mg/L (**Fig. 26**). Maximum unconsumed acid concentration in the effluent samples reached 2.4 wt% equivalent HCl (**Fig. 27**). The percentage of iron recovered in the effluent samples was 89.25 %.

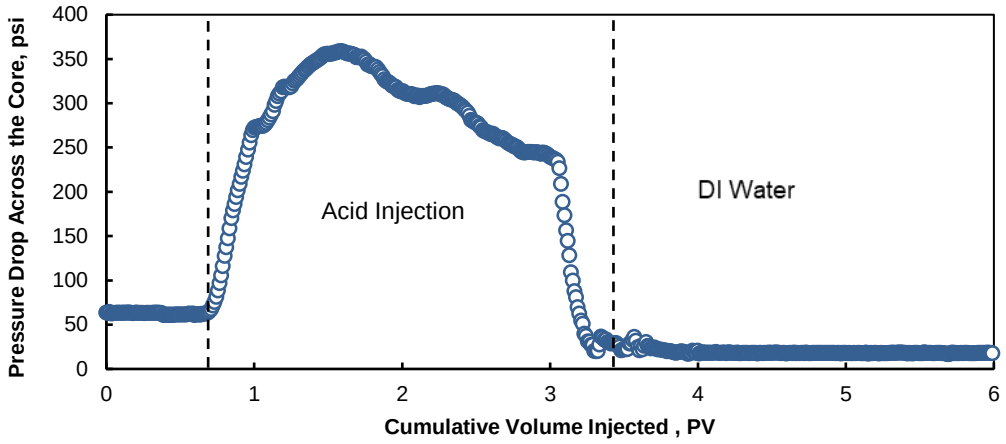

Fig. 24: Pressure drop across the core for acid injection at 5 cm^3/min as a function of the cumulative volume injected at 150°F.

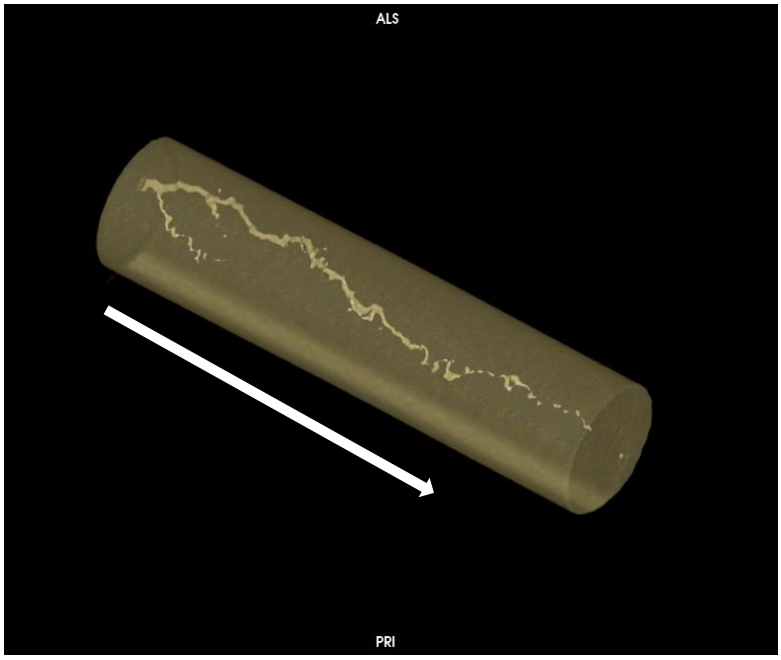

Fig. 25: CT scan image of Indiana limestone after acidizing at 5 cm^3/min.

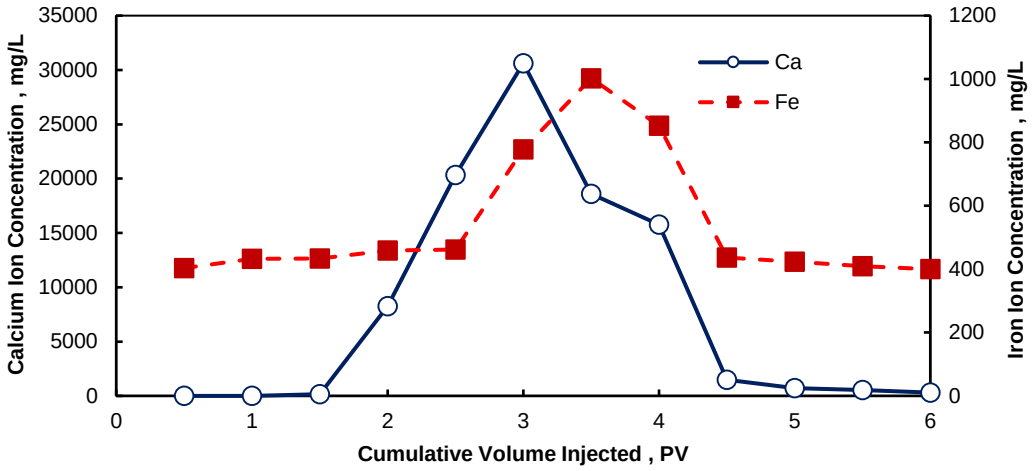

Fig. 26: Calcium and Iron ion concentration for the acid injection at 5 cm^3/min as a function of the cumulative volume injected at 150°F.

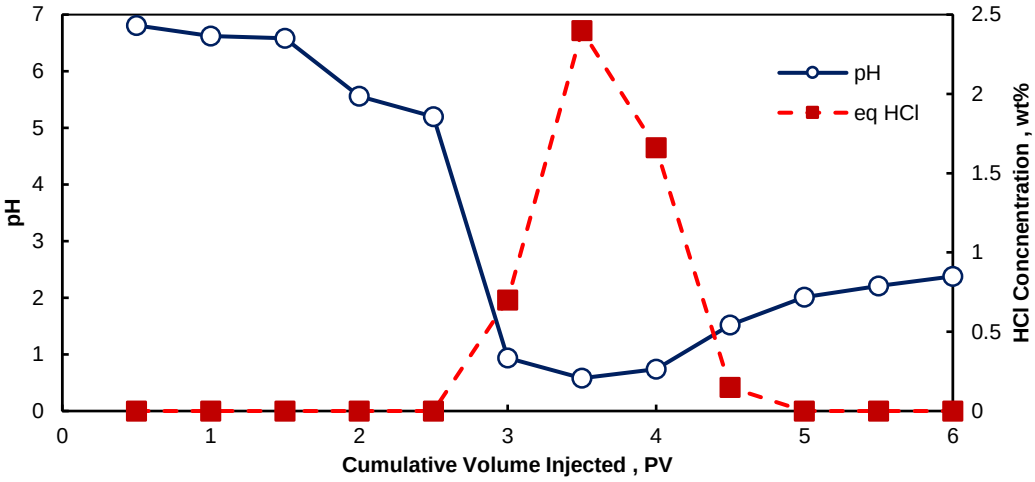

Fig. 27: Acid concentration in terms of equivalent HCl and pH of core effluent samples for the acid injection at 5 cm^3/min as a function of the cumulative volume injected at 150°F.

VII.3.3 Impact of Temperature

The impact of temperature on the process of diversion was investigated by injecting the in-situ gelled acid at 5 cm^3/min and 250^oF. About 1.25 PV of acid was injected before breakthrough was observed. This is significantly lower compared to the volume of acid required to breakthrough for the 150^oF case. The increase in temperature lowers the apparent viscosity of both live and partially spent in-situ gelled acid. The lowered viscosity allows better transport of the acid to the rock causing more reaction. The pressure drop across the core increased immediately when acid entered the core (**Fig. 28**). However, only few pressure oscillations were observed before acid breakthrough, which indicated that at the higher temperature the gel did not develop enough viscoelastic strength to generate significant diversion. CT scan images (**Fig. 29**) indicated that there was no significant tortuosity observed in the wormhole generated.

The increase in temperature also increases the rate of reaction of the acid with the core. This is observed in the higher maximum calcium ion concentration of 48,000 mg/L in the effluent samples (**Fig. 30**). Material balance studies indicated that there was a recovery of 90.8% of the iron injected in the effluent samples. The maximum unreacted acid concentration of 1.86 wt% equivalent HCl (**Fig. 31**).

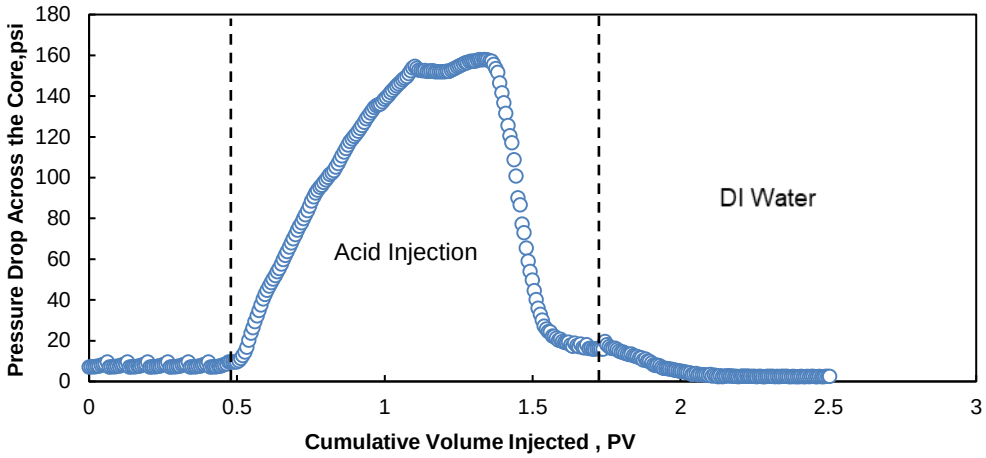

Fig. 28: Pressure drop across the core for the acid injection at 5 cm^3/min as a function of the cumulative volume injected at 250°F.

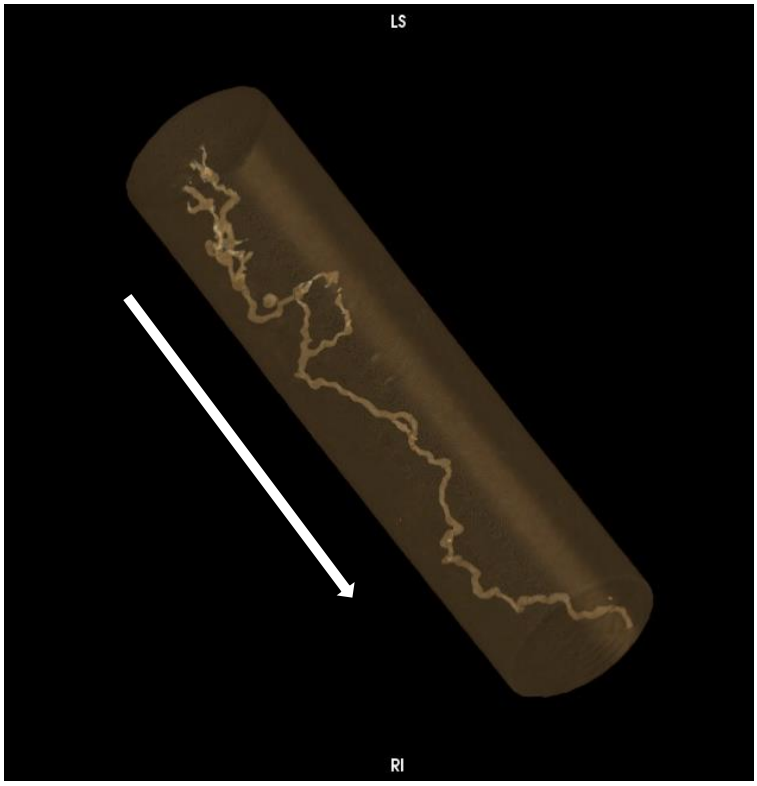

Fig. 29: CT scan image of Indiana limestone after acidizing at 5 cm^3/min and 250°F.

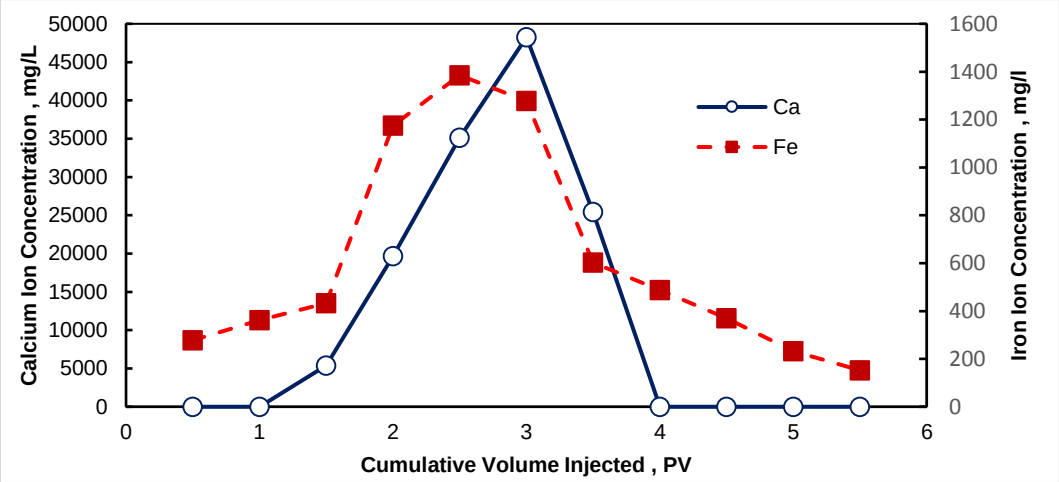

Fig. 30: Calcium and Iron ion concentration for the acid injection at 5 cm^3/min as a function of the cumulative volume injected at 250°F.

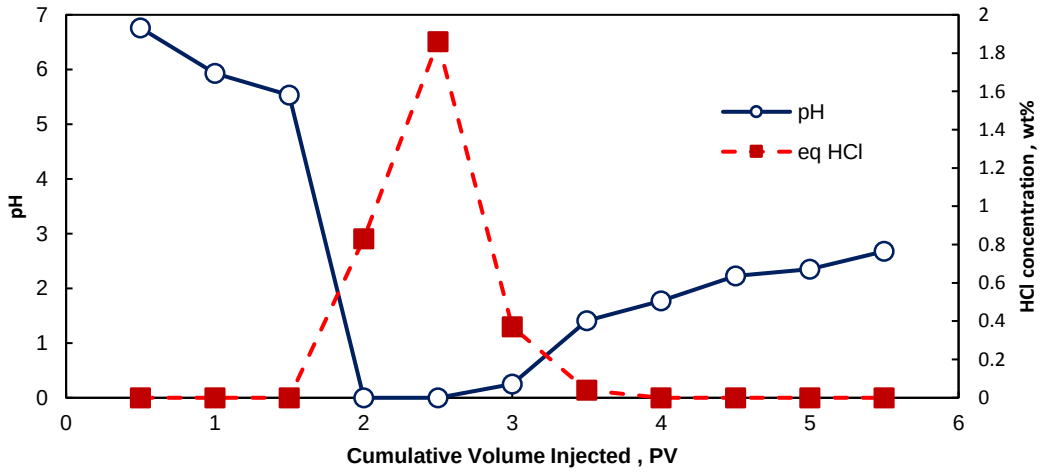

Fig. 31: Acid concentration in terms of equivalent HCl and pH of core effluent samples for the acid injection at 5 cm^3/min as a function of the cumulative volume injected at 250°F.

VII.3.4 Summary

The in-situ gelled acid clearly demonstrated a capacity for diversion of acid in a carbonate reservoir. In each of the coreflood tests that were conducted, the wormholes generated by the in-situ gelled acid were characterized and found to have significant tortuosity. The impact of flow rate on the diversion process was investigated. $5cm^3$/min was found to be optimal injection rate with minimum acid volume required for breakthrough and maximum unreacted acid at breakthrough. The polymer-based acid gel system was found to have successfully generate wormholes in cores with permeability as low as 10 mD indicating no damage caused by filtration of polymer. The in-situ gelled acid system was also successful in generating a wormhole with tortuosity at temperatures upto 250^oF. In all the coreflood tests conducted, there was no indication of any damage caused by precipitation of iron. On an average 90% of the injected iron was recovered in the effluent samples.

VII.4 Dual Coreflood Studies

Acid diversion process is greatly impacted by the contrast in permeability in the reservoir. Dual coreflood studies were conducted to investigate the impact of permeability contrast on the diversion caused by the in-situ gelled acid. The tests involved injection of 1 PV of in-situ gelled acid followed by the injection of 1 PV of 15 wt % HCl. DI water was injected until the pressure drop across both the cores stabilized. The effluent samples were collected for both cores and were analyzed for the rate of the fluid collected. A total of 3 dual coreflood tests were conducted.

VII.4.1 Impact of Permeability Contrast

Three coreflood experiments were performed at the permeability contrast of around 2.5, 5, and 7.5. These tests were conducted at 150^{o}F.

Low Permeability Contrast (1:3)

In this experiment, cores 125 and 131 of initial permeability 58.9 and 19.7 mD were tested for acid diversion at an injection rate of 5 cm^3/min. **Fig. 32** and **33** shows the pressure drop across the high permeability core and the effluent collection rate across both the cores. Prior to the injection of acid, the effluent collection rate was 4.15 and 1.85 cm^3/min for cores 125 and 131 respectively. As the in-situ gelled acid entered the core, the pressure drop increased to 70 psi while the effluent collection rate of core 125 decreased to a value of 3.2 cm^3/min and an increase in core 131 to a value of 2.8 cm^3/min. The increased flow for core 131 was because the higher permeability core 125 was

plugged by the acid causing the fluid to divert to the lower permeability core 131. When HCl injection was carried out, a slight increase in pressure was observed which was followed by a significant decline in pressure which indicated breakthrough. An enhancement in permeability enhancement was observed in both cores in the CT scan images (**Fig. 34**), with breakthrough in core 125 and a wormhole of significant length developed in the lower permeability core 131. Although, no breakthrough was observed in the lower permeability core 131, because the wormhole propagated almost to the end of the core it was concluded that the diversion of acid was successful.

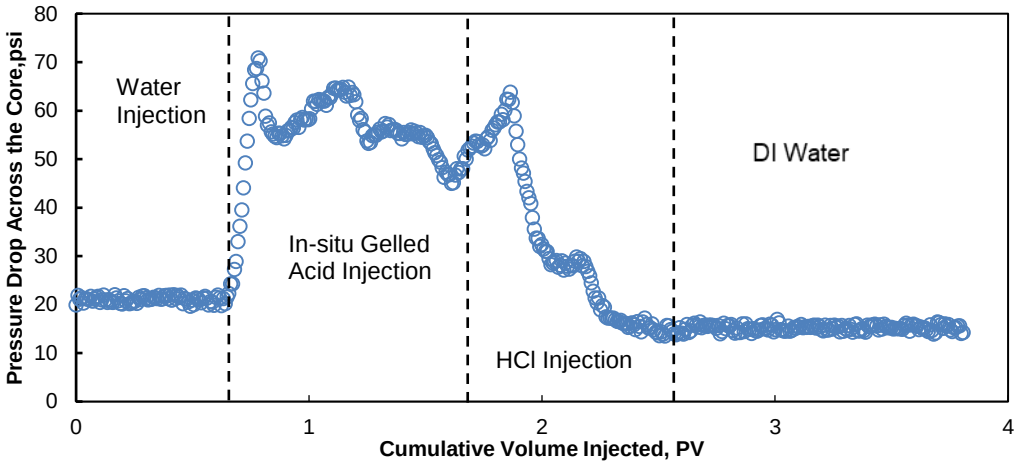

Fig. 32: Pressure drop across core 125, during multistage acid injection at 5 cm^3/min and 150°F.

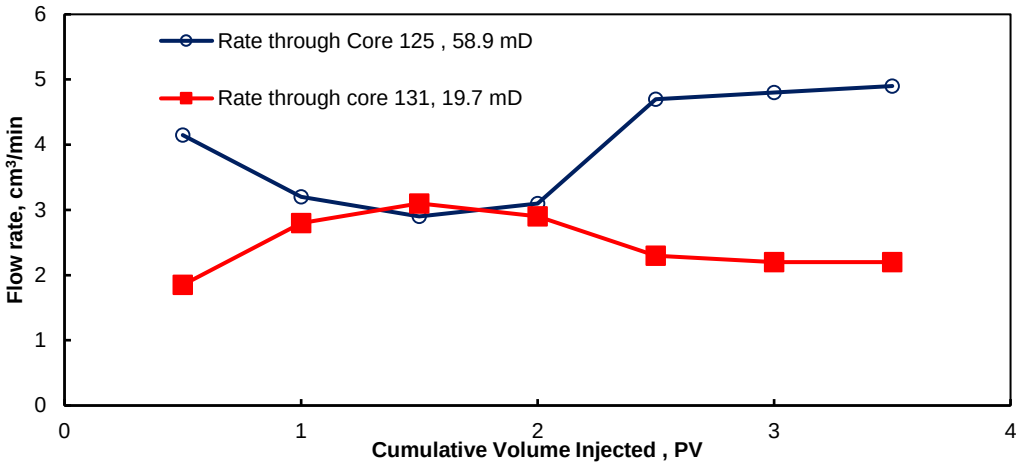

Fig. 33: Effluent collection rate across core 125 and 131 during multistage acid injection at 5 cm^3/min and 150°F.

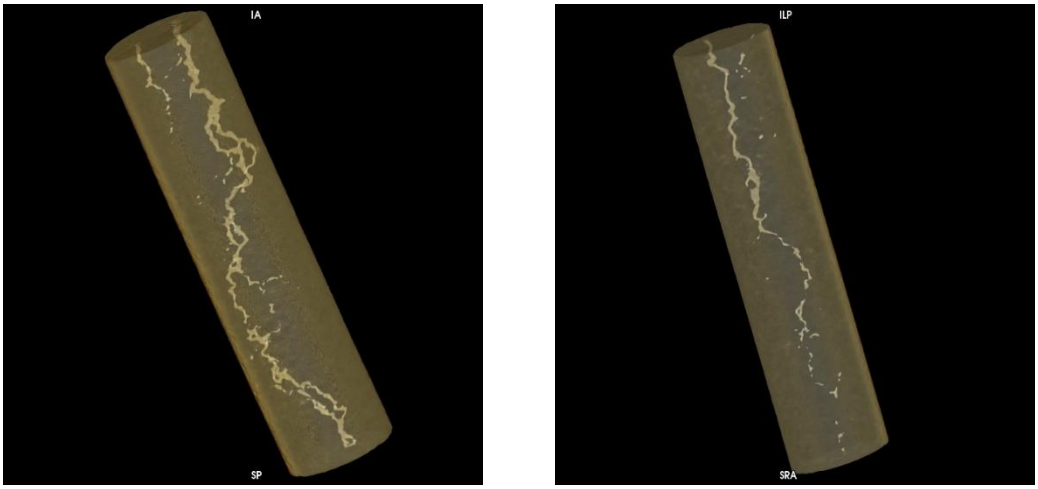

Fig. 34: CT scans for core 125 and 131 respectively after injection of multistage acid at 5cm^3/min and 150°F.

Medium Permeability Contrast (1:4.6)

Two cores, 133 and 139, of initial permeability 103.6 and 22.5 mD respectively were injected at a rate of 5 cm^3/min. **Fig. 35** show the pressure drop across the high permeability core while the effluent collection rate from both the cores is represented in **Fig. 36.** Prior to acid injection, the effluent flow rate was 4.83 cm^3/min and 1.1 cm^3/min for the cores 133 and 139 respectively. On the injection of the acid, the pressure drop increased to 113 psi with the flow rate across 133 declining to 2.9 cm^3/min and the flow rate across 139 increasing to a value of 3.4 cm^3/min. The improvement in the effluent collection rate from the low permeability core post acid injection is an indication that there was acid diverted to it. HCl injection saw the pressure stabilized for 0.2 PV before declining. CT scan analysis indicated that there was a breakthrough in the lower permeability core while the wormhole propagated to a significant distance into the higher permeability core 133 (**Fig. 37**). This indicated that the in-situ gelled acid system could successfully divert the acid from the higher to the lower permeability core.

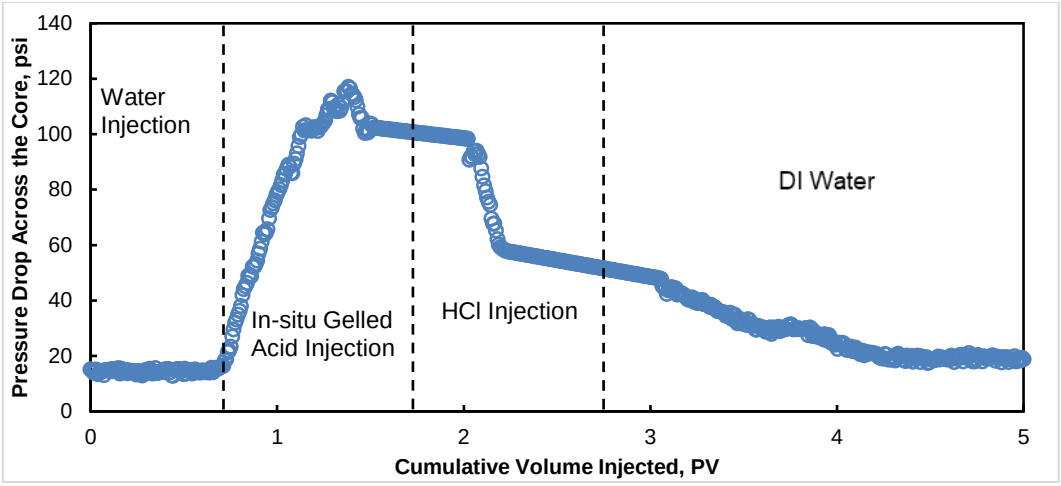

Fig. 35.: Pressure drop across core 133, during multistage acid injection at 5 cm^3/min and 150°F.

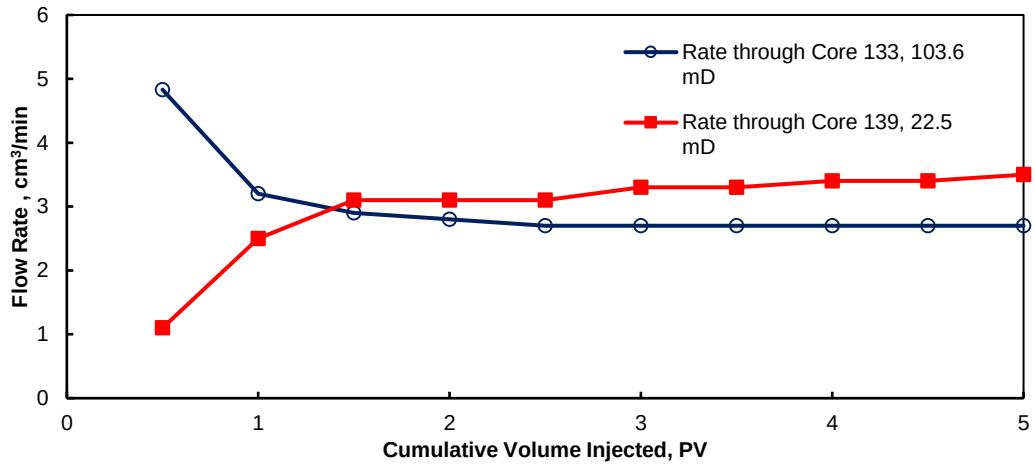

Fig. 36: Effluent collection rate across core 133 and 139 during multistage acid injection at 5 cm^3/min and 150°F.

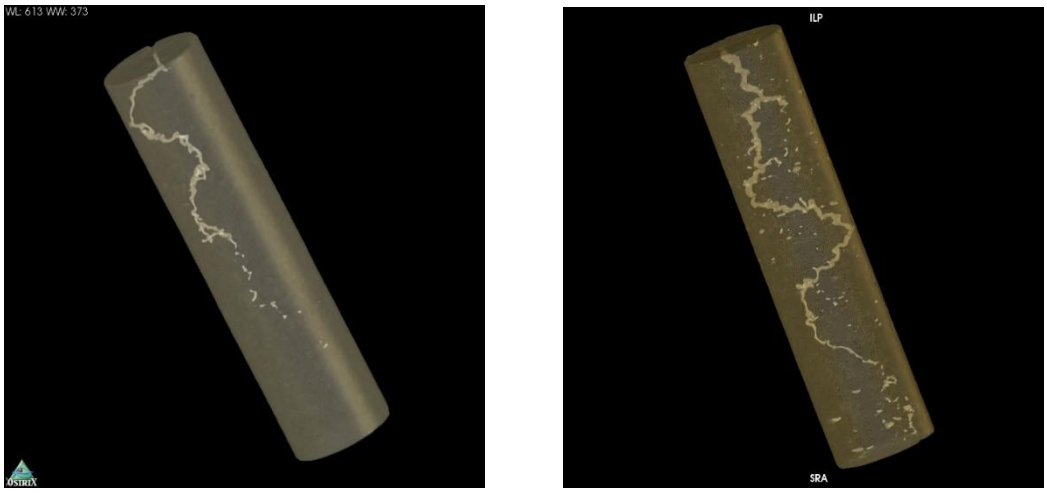

Fig. 37: CT scans for core 133 and 139 respectively after injection of multistage acid at 5cm^3/min and 150^{o}F.

High Permeability Contrast (1:8.8)

In this experiment, cores 128 and 111, with permeabilities of 63.2 and 7.19 mD respectively were injected with 1 PV each of in-situ gelled acid and 15 wt% HCl at the rate of 5 cm^3/min. The pressure drop across the core 128 was recorded in **Fig. 38**, while the effluent collection rate from both the cores was shown in **Fig. 39**. Prior to acid injection, the flow rate of effluents through cores 128 and 111 were 6.32 and 0.85 cm^3/min respectively. On injection of the in-situ gelled acid, the pressure drop across the high permeability core increased instantly to 65 psi with the effluent collection rates for core 125 declined upto 2.36 cm^3/min. There was no improvement in the effluent collection rate from core 111 which indicated that there was no flow of fluid into the lower permeability core. HCl injection lead to an immediate major decline in the pressure across the core indicating breakthrough and improvement in the fluid collection rate from core 125. CT scan images (**Fig. 40**) confirmed that there was a breakthrough of the acid in the higher

permeability core 125 while the wormhole barely propagated in the lower permeability core 111. Thus, there was no diversion observed in this case.

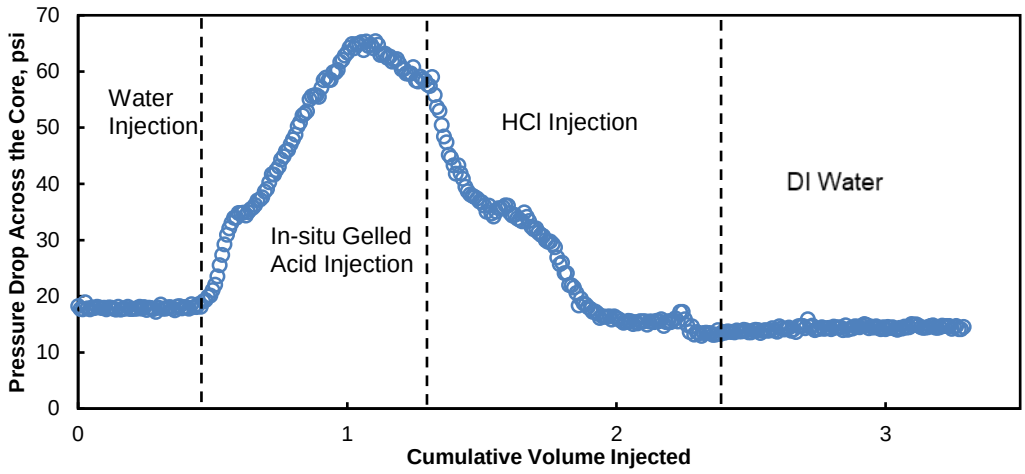

Fig. 38: Pressure drop across core 128, during multistage acid injection at 5 cm^3/min and 150°F.

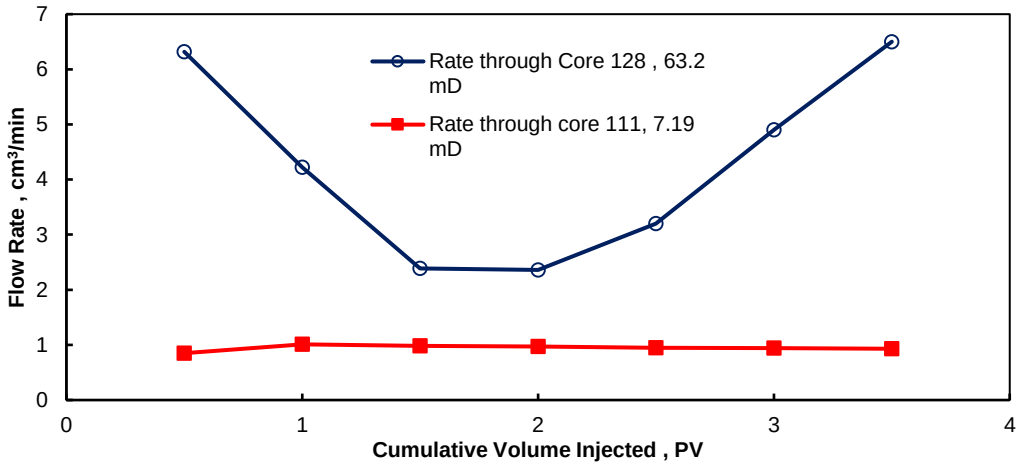

Fig. 39: Effluent collection rate across core 128 and 111 during multistage acid injection at 5 cm^3/min and 150°F.

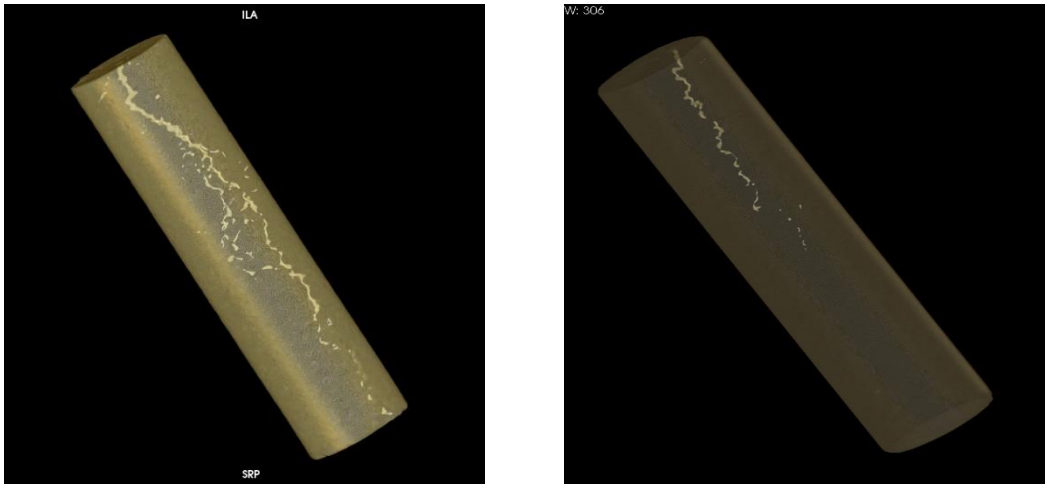

Fig. 40: CT scans for core 128 and 111 respectively after injection of multistage acid at 5cm^3/min and 150^{o}F.

Summary

The in-situ gelled acid was investigated for its ability to divert acid from the higher permeability regions of the carbonate reservoir to the lower permeability zones. The tests were conducted over three different permeability contrast ratios: 3, 4.6, and 8.8 at a flow rate of 5 cm^3/min and at 150^{o}F. The tests provided conclusive evidence that permeability contrast ratios play a very important role in the process of diversion. The in-situ gelled acid system was found to have successfully acted as an acid diversion system at permeability contrasts of up to 4.6. The low permeability cores in this case either had a breakthrough or the wormhole length was almost comparable to the wormhole in the higher permeability core.

CHAPTER VIII

CONCLUSIONS

Results of this research led to the following conclusions:

1. The in-situ gelled acid was a non-Newtonian fluid, with shear rate dependent viscosity. The spending of acid led to an increase in viscosity from pH 2 to 4.5, after which the fluid broke down without a breaker.
2. The spending of the acid led to a significant increase in the elastic modulus of the in-situ gelled acid, which demonstrated the ability of the fluid system to form a strong gel which would divert the following acid stages to the low permeability zones in the reservoir.
3. Salt concentration was found to have an impact on the viscosity of the in-situ gelled acid system. The presence of salt was found to have modified the configuration of the polymer and cause it to separate out of the acid system.
4. The acid concentration should be limited to a maximum of 5 wt%. Higher concentration of acid is expected to release more of calcium ions on reaction with the carbonate rock and the presence of excess calcium ions would lead to a lower viscosity of the acid-gel system.
5. Coreflood studies indicated that the process of diversion was greatly dependent on the injection flow rate. An optimal flow rate of 5 cm^3/min was found to require the least acid volume to breakthrough with the maximum unreacted acid in the effluent samples.

6. The in-situ gelled acid system was found to have successfully caused diversion in Indiana limestone cores of permeability as low as 10 mD. Typical problems of polymer and iron precipitation were not observed with this fluid system.
7. Dual coreflood studies indicated that the permeability contrast of the low and high zones of the reservoir had a significant impact on the process of diversion. The acid system was found to have successfully caused diversion with permeability contrasts of up to 4.6.
8. This research lead to the development of a novel cationic polymer based in-situ gelled acid system that could be used for acid diversion in medium range permeability contrast limestone reservoirs at temperatures up to 250^{o}F. This system did not exhibit any of the problems that are typically associated with polymer-acid systems: precipitation of polymer and iron. Self-breaking ability of the acid system is also an additional benefit as it saves money by eliminating the requirement of a breaker from the acid system.

REFERENCES

Ahmed, W. A. F., Nasr-El-Din, H. A., Moawad, T. M., & Elgibaly, A. A. M. (2008). Effects of Crosslinker Type and Additives on the Performance on In-Situ Gelled Acids. Paper presented at the SPE International Symposium and Exhibition on Formation Damage Control, Lafayette, Louisiana, USA.

Bazin, B. (2001). From matrix acidizing to acid fracturing: a laboratory evaluation of acid/rock interactions. *SPE Production & Facilities*, 16(01), 22-29.

Bazin, B., Charbonnel, P., & Onaisi, A. (1999). Strategy Optimization for Matrix Treatments of Horizontal Drains in Carbonate Reservoirs, Use of Self-Gelling Acid Diverter. Paper presented at the SPE European Formation Damage Conference, The Hague, Netherlands.

Bryant, S. L., & Buller, D. C. (1990). Formation Damage From Acid Treatments. doi:10.2118/17597-PA

Church, D. C., Quisenberry, J. L., & Fox, K. B. (1981). Field Evaluation of Gelled Acid for Carbonate Formations. doi:10.2118/9753-PA

Conway, M. W., Asadi, M., Penny, G. S., & Chang, F. (1999). A Comparative Study of Straight/Gelled/Emulsified Hydrochloric Acid Diffusivity Coefficient Using Diaphragm Cell and Rotating Disk. Paper presented at the SPE Annual Technical Conference and Exhibition, Houston, Texas.

Coulter, G. R., & Jennings, A. R., Jr. (1999). A Contemporary Approach to Matrix Acidizing. doi:10.2118/56279-PA

Cunningham, W. C., & Smith, D. K. (1968). Effect of Salt Cement Filtrate on Subsurface Formations. doi:10.2118/1920-PA

Deysarkar, A. K., Dawson, J. C., Sedillo, L. P., & Davis, S. K. (1984). Crosslinked Acid Gel. doi:10.2118/84-01-01

Gomaa, A. M., Mahmoud, M. A., & Nasr-El-Din, H. A. (2011). Laboratory Study of Diversion Using Polymer-Based In-Situ-Gelled Acids. doi:10.2118/132535-PA

Gomaa, A. M., & Nasr-El-Din, H. A. (2010 a). Rheological Properties of Polymer-Based In-Situ Gelled Acids: Experimental and Theoretical Studies. Paper presented at the SPE Oil and Gas India Conference and Exhibition, Mumbai, India.

Gomaa, A. M., & Nasr-El-Din, H. (2010 b). Rheological and Core Flood Studies of Gelled

and In-Situ Gelled Acids. Paper presented at the North Africa Technical Conference and Exhibition, Cairo, Egypt.

Gomaa, A. M., & Nasr-El-Din, H. A. (2010 c). New Insights Into the Viscosity of Polymer-Based In-Situ-Gelled Acids. doi:10.2118/121728-PA

Haldar, S., Nainwal, S. P., De, S. K., & Karmakar, G. P. (2004). In-situ Cross-linking Acid Diverting Agent (ISCADA): A new solution to stimulate multi-layered reservoirs. Paper presented at the SPE Asia Pacific Oil and Gas Conference and Exhibition, Perth, Australia.

Hill, D. (2005). Gelled Acid: Google Patents.

Hoefner, M., & Fogler, H. S. (1988). Pore evolution and channel formation during flow and reaction in porous media. *AIChE Journal*, 34(1), 45-54.

Hosseinzadeh, B., Bazargan, M., Rostami, B., & Ayatollahi, S. (2017). Modeling of Wormhole Propagation in Carbonate Rocks by Use of In-Situ-Gelled Acids. doi:10.2118/186101-PA

Houchin, L. R., Dunlap, D. D., & Hutchinson, J. E. (1988). Formation Damage During Gravel-Pack Completions. Paper presented at the SPE Formation Damage Control Symposium, Bakersfield, California.

Johnson, D. E., Fox, K. B., Burns, L. D., & O'Mara, E. M. (1988). Carbonate Production Decline Rates Are Reduced Through Improvements in Gelled Acid Technology. Paper presented at the Permian Basin Oil and Gas Recovery Conference, Midland, Texas.

Kalfayan, L. J., & Martin, A. N. (2009). The Art and Practice of Acid Placement and Diversion: History, Present State, and Future. Paper presented at the SPE Annual Technical Conference and Exhibition, New Orleans, Louisiana.

Klotz, J. A., Krueger, R. F., & Pye, D. S. (1974). Maximum Well Productivity in Damaged Formations Requires Deep, Clean Perforations. Paper presented at the SPE Symposium on Formation Damage Control, New Orleans, Louisiana.

Lakatos, I., & Lakatos-Szabó, J. (2004). Diffusion of H+, H2O and D2O in polymer/silicate gels. Colloids and Surfaces A: Physicochemical and Engineering Aspects, 246(1-3), 9-19.

Leontaritis, K. J. (1989). Asphaltene Deposition: A Comprehensive Description of Problem Manifestations and Modeling Approaches. Paper presented at the SPE Production Operations Symposium, Oklahoma City, Oklahoma.

Lynn, J. D., & Nasr-El-Din, H. A. (2001). A Core Based Comparison Of The Reaction Characteristics Of Emulsified And In-Situ Gelled Acids In Low Permeability, High Temperature, Gas Bearing Carbonates. Paper presented at the SPE International Symposium on Oilfield Chemistry, Houston, Texas.

MaGee, J., Buijse, M. A., & Pongratz, R. (1997). Method for Effective Fluid Diversion when Performing a Matrix Acid Stimulation in Carbonate Formations. Paper presented at the Middle East Oil Show and Conference, Bahrain.

Maheshwari, P., Maxey, J., & Balakotaiah, V. (2016). Reactive-Dissolution Modeling and Experimental Comparison of Wormhole Formation in Carbonates with Gelled and Emulsified Acids. doi:10.2118/171731-PA

McLeod, H. O. (1984). Matrix Acidizing. doi:10.2118/13752-PA

Mohamed, S. K., Nasr-El-Din, H. A., & Al-Furaidan, Y. A. (1999). Acid Stimulation of Power Water Injectors and Saltwater Disposal Wells in a Carbonate Reservoir in Saudi Arabia: Laboratory Testing and Field Results. Paper presented at the SPE Annual Technical Conference and Exhibition, Houston, Texas.

Muecke, T. W. (1982). Principles of Acid Stimulation. Paper presented at the International Petroleum Exhibition and Technical Symposium, Beijing, China.

Nasr-El-Din, H. A., Hill, A. D., Chang, F. F., & Sultan, A. S. (2007). Chemical Diversion Techniques Used for Carbonate Matrix Acidizing: An Overview and Case Histories. Paper presented at the International Symposium on Oilfield Chemistry, Houston, Texas, U.S.A.

Norman, L. R., Conway, M. W., & Wilson, J. M. (1984). Temperature-Stable Acid-Gelling Polymers: Laboratory Evaluation and Field Results. doi:10.2118/10260-PA

Patil, P. R., Sarda, A., George, S., Choudhary, Y. K., & Kalgaonkar, R. (2012). Non-Iron-Based Composition for In-situ Crosslinked Gelled Acid System. Paper presented at the SPE International Production and Operations Conference & Exhibition, Doha, Qatar.

Rabie, A. I., Gomaa, A. M., & Nasr-El-Din, H. A. (2011). Reaction of In-Situ-Gelled Acids With Calcite: Reaction-Rate Study. doi:10.2118/133501-PA

Reed, M. G. (1989). Formation Damage Prevention During Drilling and Completion. Paper presented at the SPE Centennial Symposium at New Mexico Tech, Socorro, New Mexico.

Saxon, A., Chariag, B., & Rahman, M. R. A. (2000). An Effective Matrix Diversion Technique for Carbonate Formations. doi:10.2118/62173-PA

Taylor, K. C., & Nasr-El-Din, H. A. (2003). Laboratory Evaluation of In-Situ Gelled Acids for Carbonate Reservoirs. doi:10.2118/87331-PA